



Article

Streamflow Decline in the Yellow River along with Socioeconomic Development: Past and Future

Shi Lun Yang ^{1,*}, Benwei Shi ¹, Jiqing Fan ¹, Xiangxin Luo ², Qing Tian ³, Haifei Yang ⁴, Shenliang Chen ¹, Yingxin Zhang ¹, Saisai Zhang ⁵, Xuefa Shi ⁶ and Houjie Wang ^{7,8}

¹ State Key Laboratory of Estuarine and Coastal Research, East China Normal University, Shanghai 200062, China; bwshi@sklec.ecnu.edu.cn (B.S.); jqfan1992@163.com (J.F.); slchen@sklec.ecnu.edu.cn (S.C.); 51193904011@stu.ecnu.edu.cn (Y.Z.)

² Institute of Estuarine and Coastal Research, Sun Yat-sen University, Guangzhou 510275, China; luoxx6@mail.sysu.edu.cn

³ School of Marine Science, Nanjing University of Information Science and Technology, Nanjing 210044, China; 002757@nuist.edu.cn

⁴ Survey Bureau of Hydrology and Water Resources of the Changjiang Estuary, Bureau of Hydrology, Changjiang Water Resources Commission, Shanghai 200136, China; hfyang1991@163.com

⁵ Shanghai Waterway Engineering Design and consulting Co., Ltd., Shanghai 200120, China; zhangsaisai@shiw.com.cn

⁶ Key Laboratory of Marine Sedimentology & Environmental Geology, First Institute of Oceanography, State Oceanic Administration, Qingdao 266061, China; xfshi@fio.org.cn

⁷ Key Laboratory of Submarine Geosciences and Prospecting Techniques, College of Marine Geosciences, Ocean University of China, 238 Songling Rd., Qingdao 266100, China; hjwang@mail.ouc.edu.cn

⁸ Laboratory for Marine Geology, Qingdao National Laboratory for Marine Science and Technology, Qingdao 266061, China

* Correspondence: slyang@sklec.ecnu.edu.cn

Received: 28 January 2020; Accepted: 6 March 2020; Published: 14 March 2020



Abstract: Human society and ecosystems worldwide are increasingly threatened by water shortages. Despite numerous studies of climatic impacts on water availability, little is known about the influences of socioeconomic development on streamflow and water sustainability. Here, we show that the streamflow from the Yellow River to the sea has decreased by more than 80% in total over the last 60 years due to increased water consumption by agricultural, industrial and urban developments (76% of the streamflow decrease, similarly hereinafter), decreased precipitation (13%), reservoir construction (6%) and revegetation (5%). We predict that if the past trends in streamflow will continue, year-round dry-up in the lower Yellow River will commence in the late 2020s or early 2030s, unless effective countermeasures such as water diversion from the Yangtze River are taken. These results suggest that streamflow in semiarid basins is highly vulnerable to human impacts and that streamflow decline would in turn hinder further socioeconomic development and endanger river-sea ecosystems.

Keywords: streamflow; water resource; socioeconomic development; Yellow River

1. Introduction

The decline of freshwater sources is fatal for human water security and ecosystem sustainability. Human society and ecosystems are increasingly threatened by water shortages, despite the global abundance and the renewable character of this resource [1–4]. For example, the water discharge to the Sea from the Nile decreased to null after the construction of the Aswan High Dam and increased water extraction for agriculture development [5]. A similar situation was reported in the Colorado

River [6]. Dramatic streamflow decline has also occurred in the Indus River and the Rio Grande River [6]. This circumstance is primarily caused by the heterogeneous distribution of freshwater in the world and time [2,7] and the increased water demand with increased socioeconomic development. To develop strategies to cope with water shortages, we must first identify the underlying causes of water shortages at global, regional and local scales. Numerous studies have been conducted on the climatic influences on water resources at decadal scales, and great uncertainties in precipitation trends and water availability have been found [8–12]. In comparison, less is known about the water scarcity caused by human activities [11], especially research including assessment of streamflow decline due to socioeconomic growth in arid and semiarid basins.

Rivers provide the primary route for continental water circulation and the major link between land and sea [6]. Most global cities and wetlands are distributed along rivers and in river deltas. Streamflow is the amount of water passing through a river section in a unit time. Streamflow change has great socioeconomic and ecological implications. Although water stored in lakes and reservoirs can assist in increasing water availability for human society, streamflow is the main focus of water resource assessments [13]. Thus, human impacts on streamflow should be a key research point for the sustainable utilization of water resources.

The Yellow River (YR) (Figure 1) is known as the “Mother River of Chinese Civilization”. The YR flows across nine provinces in China, and the mainstem length is 5500 km. The YR Basin (YRB) area is 750,000 km², and the population in the YRB was 110 million people in 2016. The population density in the YRB is 2.7 times higher than the world average. The long-term mean precipitation within this basin (460 mm/yr) is much lower than the global average (950 mm/yr), and the long-term mean potential evaporation (1690 mm/yr) is significantly higher than the global average (1150 mm/yr). These water-limiting conditions lead to a runoff per capita in the YRB is only 1/9th of the world average (Table A1). Moreover, this basin has experienced rapid socioeconomic growth since the 1980s. It is therefore necessary to explore whether streamflow is vulnerable to socioeconomic development and to attempt to determine whether this streamflow will be able to adequately support socioeconomic and ecosystem sustainability in the future. These issues may have global implications, especially for other arid or semiarid basins that are experiencing rapid socioeconomic development.

Numerous studies have examined the climatic and anthropogenic contributions to the streamflow decline in the YR. For example, 75% of the streamflow decline in the upper YR between 1956 and 2000 was attributed to decreased precipitation, whereas 25% of the streamflow decline was ascribed to human activities; meanwhile, 57% and 43% of the streamflow decrease in the middle YR were attributed to precipitation decline and human activities, respectively [14]. Similarly, in the Weihe River, a tributary in the middle reaches of the YR, the streamflow decline during 1960–2009 was mainly attributed to climate change, while human activities were also responsible [15]. In contrast, 70% and 30% of the streamflow decline in the middle reaches of the YR from 1957 to 2010 were attributed to soil conservation measures and precipitation reduction [16]. Within the catchment, excluding the headwater areas, which cover ~30% of the YR length, water consumption contributed more than 90% to streamflow reduction between the 1950s and the 1980s; afterwards, land cover change became the major factor of streamflow decrease—since 2000, government management schemes have prevented streamflow from declining further and guarantee its stability [17]. For the entire YRB, precipitation decline and human activities were responsible for 51% and 49% of the streamflow decrease between 1950 and 2000 [18]. In comparison, human activities were responsible for 73% of the streamflow decrease from 1960–1979 to 1980–2000, and for 83% of the decreased streamflow during 2001–2014 [19]. However, the results and conclusions of the previous studies are highly varied, probably because of the differences in study area, study period and methodology. In addition, little has been done in quantificationally predicting the future trend of the YR streamflow on the basis of analysis of the already existing streamflow trend, systematic quantification of the impacts of major driving factors on the streamflow, and evaluation of the future scenarios of the major driving factors. There is an urgent need to investigate the near future trend of the YR streamflow, considering that the annual

streamflow has drastically decreased [19–22] and seasonal dry-up in the lower YR once frequently occurred [23,24] in the past, and future water demand in the YRB can be expected to further increase with socioeconomic development [25,26].

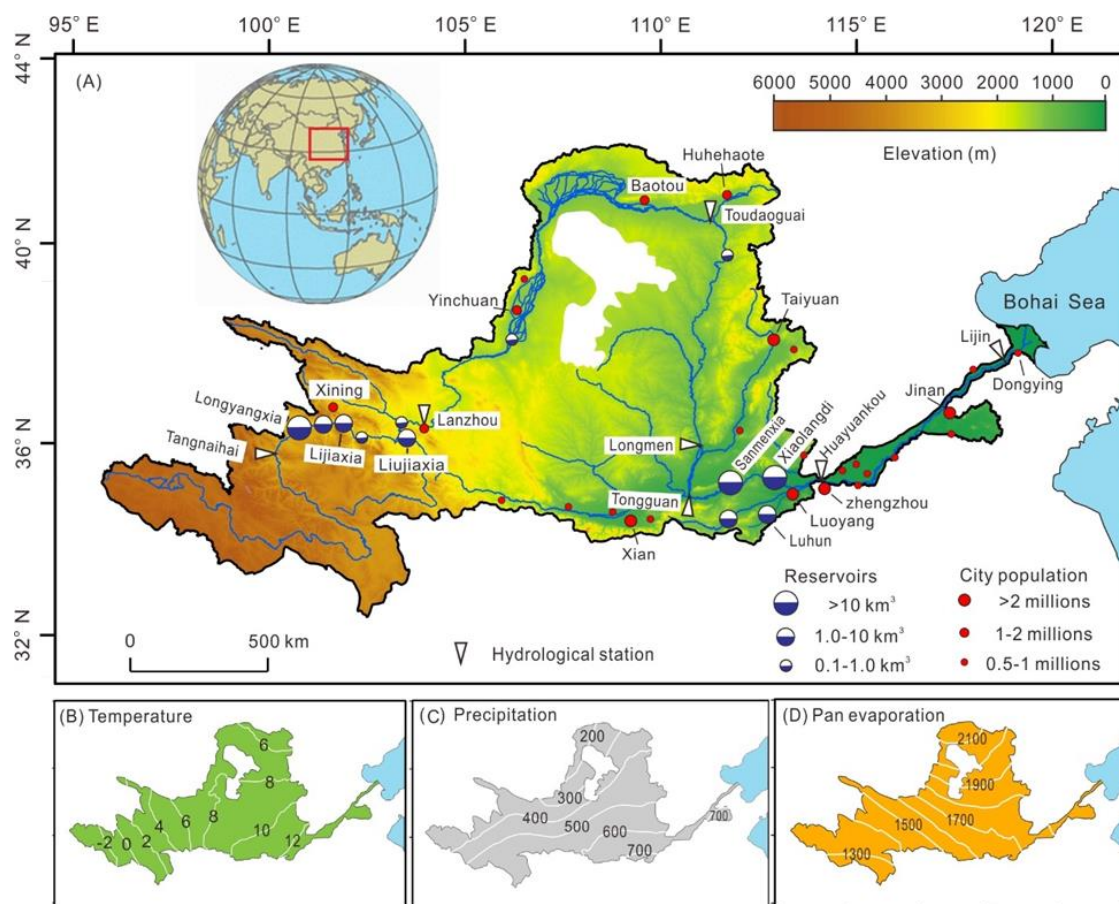


Figure 1. The Yellow River basin. (A) Elevation, river system, and major hydrological stations, reservoirs and cities (Xining, Lanzhou, Yinchuan, Huhehaote, Taiyuan, Xian, Zhengzhou and Jinan are provincial capitals). (B–D) Contours of time-averaged (1957–2016) temperature, precipitation and pan evaporation, respectively (based on data gauged at 83 stations).

In this study, we aimed to investigate quantitatively the decline trend of streamflow in the YR under climatic and anthropogenic impacts. Our objectives were to: (1) quantify the decreasing trend in annual streamflow over the past six decades; (2) evaluate the weights of major drivers in the streamflow decline; (3) predict the commence time of annual streamflow depletion under future natural and socioeconomic scenarios. Our results may add to the knowledge on streamflow vulnerability to socioeconomic development and assist in improving streamflow management for both the YR and global rivers.

2. Materials and Methods

2.1. Data Mining

Annual streamflow data, based on daily measurements following international standards at seven gauging stations from 1957–2016, were collected by the Yellow River Conservancy Commission (YRCC) of the Ministry of Water Resources of China (<http://www.yellowriver.gov.cn>). Annual water consumption data from 1955–1997 excluding 1959, 1960 and 1989 were after Miao et al. [21], whereas annual water consumption data from 1998–2016 were collected by the YRCC (<http://www>).

yellowriver.gov.cn). Annual precipitation, temperature and pan evaporation data from 82 national base meteorological stations from 1957–2016 were compiled by the National Meteorological Information Center (NMIC) of the China Meteorological Administration (<http://data.cma.gov.cn/>) and were subject to strict quality control by NMIC. The selected stations were evenly distributed within and around the study area. Data on population, grain yield and gross domestic product (GDP) from 1957–2016 were collected from the national and regional statistical yearbooks. To estimate the total population, grain yield and GDP of the catchment, we first delineated the administrative boundaries on the watershed map using the ArcGIS (Geographic Information System) 10.5 (ESRI, Redlands, CA, USA). We then calculated the area of this catchment and calculated the ratio of catchment area to administrative area for each administrative region. The products of this ratio and the regional population, grain yield and GDP were the components of the population, grain yield and GDP within the catchment, respectively. The sum of the populations from all subregions within a catchment was taken as the total population of the catchment and was similarly calculated for grain yield and GDP. The annual population, grain yield and GDP dataset from the use of this approach are highly reliable, because 72% of the involved county-level administrative regions (329 in total) are entirely within the watersheds of the YR, and 28% of them are partly distributed in the catchment of the YR (<https://baike.so.com/doc/4554089-4764686.html>). In the traditional method, the population, grain yield and GDP of the administrative regions, which stretch across the watershed boundaries, are completely included as the data in the basin. In other words, some areas beyond the watersheds were included as parts of the river basin in the traditional method. In comparison, only areas within the watersheds were included as portions of the river basin in our method. Our estimates of annual population, grain yield and GDP were somewhat smaller but more accurate than values from the traditional method. For example, our estimated catchment population in 1990 is 92 million, compared with 98 million by the traditional method (<https://baike.so.com/doc/4554089-4764686.html>). The catchment population in 2006 is 103 million by our approach, in comparison with 113 million by the traditional method [27].

2.2. Methodology

There are several types of approaches for separating the impacts of climate change and human activities on streamflow, including (1) hydrological modeling, (2) conceptual approaches (Budyko hypothesis, Tomer Schilling framework), (3) analytical approaches (climate elasticity method and hydrological sensitivity method) and (4) methods based on hydrological field data (paired catchment method, time-trend method) [28]. Although these approaches are different in principle, material and procedure, they are all useful [28]. In this study, taking the advantage of systematic data (e.g., precipitation, potential evaporation, streamflow, population, grain yield and GDP), we used the *time-trend method* for evaluating quantitatively the past trends of the variables and the contributions of major driving factors to the decline trend of streamflow, and for predicting the commencement of streamflow depletion in the future decades under scenarios of climate change and human impacts. This method is frequently employed in analysis of hydrological processes [15–17,28–30]. Without using this approach, it would be difficult for us to achieve our objectives.

2.2.1. Establishing the Temporal Trends in Measured Streamflow and Precipitation Water

The Mann–Kendall test [31,32] and regression analysis were used to analyze the temporal trends in measured annual streamflow (Q_M) and precipitation water (Q_P), where precipitation water is defined as the product of the area and area-averaged precipitation in the catchment above the gauging station (Table A2).

2.2.2. Calculating Trend-Based Changes in Streamflow and Precipitation Water over the Past Six Decades

We predicted the streamflow values in 1957 ($Q_{M\ 1957}$) and 2016 ($Q_{M\ 2016}$) at the gauging stations using the best temporal regression trend equations of annual streamflow in Table A2. For example, the

best temporal regression trend equation of annual streamflow at Lijin was $Q_M = -1344\ln(Y) + 10,235.9$ ($R^2 = 0.656$, $p < 0.0001$), where Y represents calendar year and Q_M represents the streamflow (km^3/yr) measured at Lijin in the corresponding calendar year. Based on this equation, the Q_M 1957 and Q_M 2016 were calculated to be $49.5 \text{ km}^3/\text{yr}$ and $9.6 \text{ km}^3/\text{yr}$, respectively. Subsequently, we calculated the streamflow change from 1957 to 2016 (Q_{MC} 1957–2016) as:

$$Q_{MC} \text{ 1957-2016 (\%)} = 100 (Q_M \text{ 2016} - Q_M \text{ 1957})/Q_M \text{ 1957} \quad (1)$$

where Q_{MC} 1957–2016 (%) represents the relative streamflow change from 1957 to 2016 (in unit of %). Because the values of Q_M 1957 and Q_M 2016 were 49.5 and $9.6 \text{ km}^3/\text{yr}$, Q_{MC} 1957–2016 (%) was calculated to be -81% .

Similarly, we predicted the precipitation water in 1957 (Q_P 1957) and 2016 (Q_P 2016) using the best temporal regression trend equations of annual precipitation rates for the sub-basins above the streamflow gauging stations in Table A2 and calculated the precipitation water changes (%) from 1957 to 2016 (Q_{PC} 1957–2016) as:

$$Q_{PC} \text{ 1957-2016 (\%)} = 100 (Q_P \text{ 2016} - Q_P \text{ 1957})/Q_P \text{ 1957} \quad (2)$$

2.2.3. Assessing the Contribution of Precipitation Change to the Decreased Streamflow Rate

To remove the influence of precipitation change on the streamflow, we first established correlations between annual precipitation-derived natural streamflow (Q_N) and Q_P for each sub-basin above the streamflow gauging stations for an initial period (1957–1966) ($R^2 = 0.65$ – 0.87 ; $p < 0.001$ – $p < 0.0001$), where Q_N is defined as the sum of Q_M , water consumption (W_C) and water impoundment by reservoirs, as the impacts of other human activities on streamflow were negligible in the initial period (1957–1966). Then, we predicted the Q_N values in 1957 (Q_N 1957) and 2016 (Q_N 2016) using the correlation equations between Q_N and Q_P and the values of Q_P 1957 and Q_P 2016 and modified the Q_M 2016 value by adding the difference between Q_N 1957 and Q_N 2016. After that calculation, we revised the decreased streamflow rate from:

$$Q_{M-DR} = (Q_M \text{ 2016} - Q_M \text{ 1957})/59 \quad (3)$$

To:

$$Q_{M-DR-P} = [(Q_M \text{ 2016} - Q_M \text{ 1957}) - (Q_N \text{ 2016} - Q_N \text{ 1957})]/59 \quad (4)$$

where Q_{M-DR} represents the trend-based decreased streamflow rate measured at a gauging station including the impact of precipitation change, the number 59 reflects the time length (years) from 1957 to 2016, and Q_{M-DR-P} represents the trend-based decreased streamflow rate excluding the impact of precipitation change. The difference between Q_{M-DR} and Q_{M-DR-P} reflects the contribution of precipitation change to the trend-based decreased streamflow rate.

2.2.4. Predicting Calendar Year from which Annual Streamflow Depletion Will Commence in the YR

For the scenario where the streamflow and precipitation trends in future decades will be the same as in the past six decades, we used Equation (5) to predict the calendar year from which annual streamflow depletion will commence at a gauging station (Y):

$$Y = 2016 + 59 Q_M \text{ 2016}/(Q_M \text{ 1957} - Q_M \text{ 2016}) \quad (5)$$

For the scenario where the future streamflow trend will be the same as in the past six decades, but the future precipitation trend will be stable (i.e., no increasing or decreasing trend will occur), we used Equation 6 to predict the calendar year from which annual streamflow depletion will commence at a gauging station (Y_{-P}):

$$Y_{-P} = 2016 + 59 Q_M \text{ 2016}/[(Q_M \text{ 1957} - Q_M \text{ 2016}) - (Q_N \text{ 1957} - Q_N \text{ 2016})] \quad (6)$$

For the scenario where the future streamflow trend will be the same as in the past six decades but the future precipitation trend will be inverse to the trend of the past six decades, we used Equation (7) to predict the calendar year from which annual streamflow depletion will commence at a gauging station (Y_{+P}):

$$Y_{+P} = 2016 + 59 Q_M 2016 / [(Q_M 1957 - Q_M 2016) - 2(Q_N 1957 - Q_N 2016)] \quad (7)$$

The methodology addressed above is outlined in Figure 2.

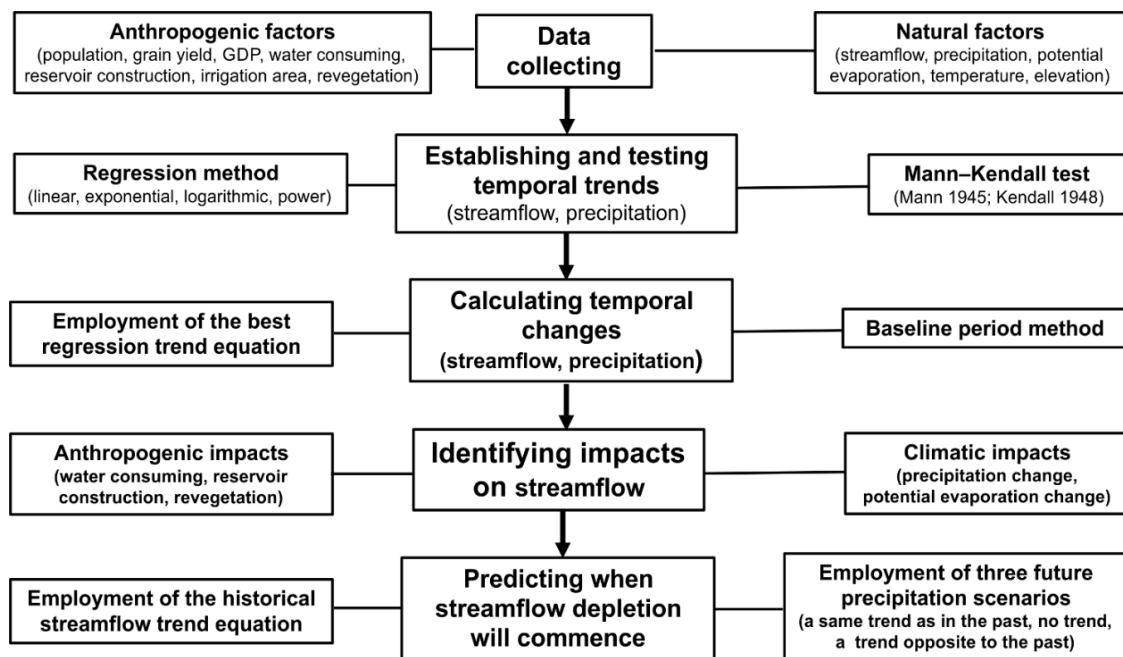


Figure 2. Flow chart of methodology.

3. Results and Discussion

3.1. Streamflow Decline over the Past Decades

From the earliest decade (1957–1966) to the latest decade (2007–2016), the time-averaged streamflow at Tangnaihai Station (Figure 1A) (1553 km from the headwater, same as below) increased by 2.0%, while the time-averaged streamflow decreased by 9.3% at Lanzhou (2096 km), 27% at Toudaoguai (3472 km), 38% at Longmen (4195 km), 44% at Tongguan (4350 km), 44% at Huayuankou (4678 km) and 64% at Lijin (5464 km) (Table 1). Although the results of linear, logarithmic, power and exponential regressions are slightly different (Table A2), decreasing trends in annual streamflow were found at all gauging stations, and the streamflow decrease was increasingly aggravated downstream from Tangnaihai (Figure 3, Table A2). According to the best of the linear, logarithmic, power and exponential regressions, the decreasing trend at Tangnaihai was nonsignificant ($R = 0.178$, $p = 0.18$), whereas the decreasing trends at other stations were all significant ($R = 0.349$ – 0.678 , $p = 0.006$ – < 0.0001) (Table A2). Thus, the decreasing streamflow trends are highly reliable except for the headwater reach where the decreasing trend is somewhat uncertain. Based on the best regression trends (Figure 2, Table A2), from 1957 to 2016, the streamflow decreased by 14% at Tangnaihai, 23% at Lanzhou, 45% at Toudaoguai, 52% at Longmen, 56% at Tongguan, 56% at Huayuankou and 81% at Lijin (tidal limit) (Figure 3, Table A2).

Table 1. Changes in amount of precipitation water and streamflow at gauging stations from the baseline decade (1957–1966) to the latest decade (2007–2016).

Variables	Tannaihai	Lanzhou	Toudaoguai	Longmen	Tongguan	Huayuankou	Lijin
Downstream distance from headwater (km)	1553	2096	3472	4195	4350	4678	5464
Precipitation water (km ³ /yr)	1957–1966	62.7	109	150	206	312	345
	2007–2016	67.2	114	145	209	305	348
	Change (%)	7.1	5.7	3.1	1.5	−2.3	−3.5
Streamflow (km ³ /yr)	1957–1966	19.6	33.4	24.8	31.6	43.7	47.5
	2007–2016	20.0	20.2	18.0	19.7	24.4	17.1
	Change (%)	2.2	−9.6	−27.1	−37.7	−44.2	64.0

Amount of precipitation water: The product of catchment area upper than the gauging station and mean precipitation of the catchment area.

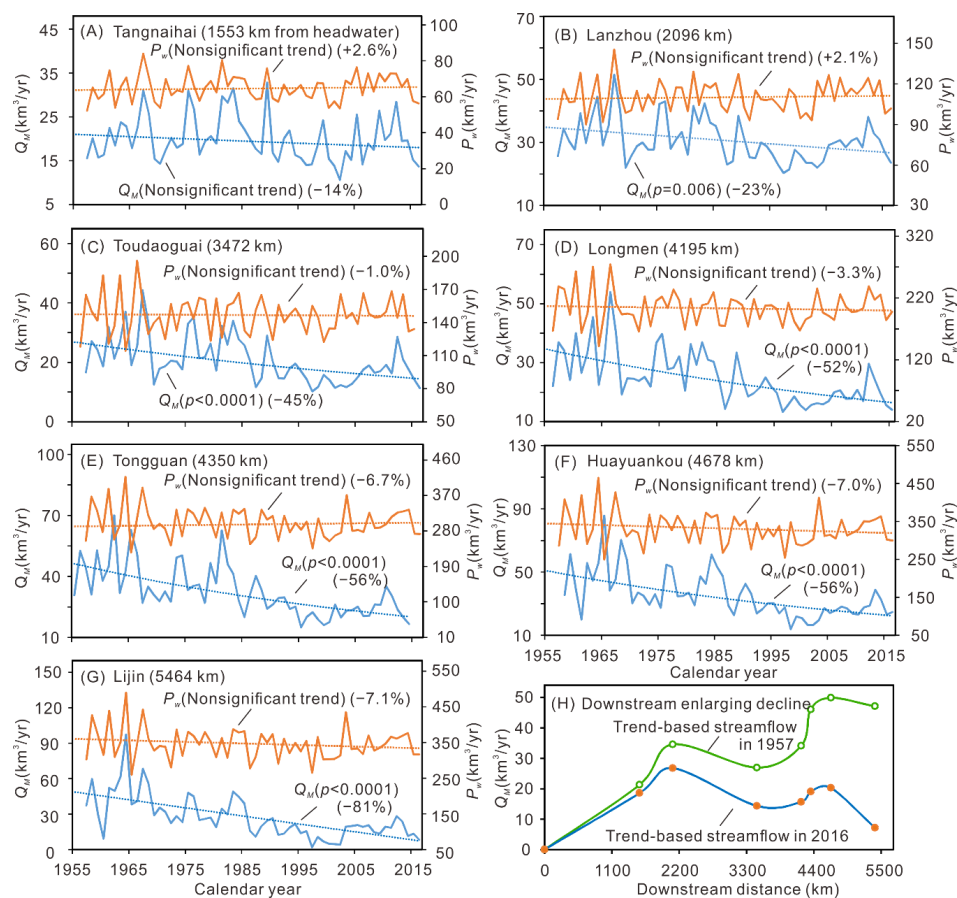


Figure 3. Temporal trends in annual precipitation water and streamflow at the gauging stations on the YR mainstem. (A–G) Time series of annual precipitation water received in the catchment upstream of the gauging station (P_w) and streamflow measured at the station (Q_M) (solid line), trendline (dashed), significance level (p) and trend-based relative change (%; positive and negative values indicating increase and decrease, respectively). The subfigure title indicates the name of the gauging station and the distance between the station and headwater. Each trendline represents the statistical equation which is highest in correlation coefficient among linear, logarithmic, power and exponential regressions. Statistical equations are shown in Table A2. (H) Downstream intensified streamflow decline. The first point represents the headwaters, and the other seven points represent the gauging stations Tangnaihai, Lanzhou, Toudaoguai, Longmen, Tongguan, Huayuankou and Lijin from upstream to downstream.

The results of the above two methods (baseline period method and statistical trend method) are somewhat different. First, the results of the baseline period method indicated a temporal increase in the streamflow at the Tangnaihai Station, whereas the results of the statistical method indicated temporal decrease in streamflow at this station. Second, for the other stations, the streamflow decreases (%) calculated by the baseline period method were lower than the streamflow decreases (%) calculated by the statistical trend method (Table 1, Table A2). These inconsistent results are attributed to differences in calculation between the two methods. Specifically, in the baseline period method, the average annual streamflow values during the earliest and latest decades were calculated and compared. In comparison, in the statistical trend method, regression trends based on the time series of annual streamflow over the 60 years were established and employed to predict the streamflow values in the earliest and latest annual years (see the methodological Section 2.2 and Table A2). The advantage of the baseline period method is effectively neutralizing the influence of the interannual changes. However, this method is unable to reflect the changes during the intervening period. In comparison, the statistical trend method can reveal the changes in the entire time series. In addition, the result of the statistical trend can be employed to predict the future streamflow tendency, if one makes the simplistic assumption that the trends of influencing factors will continue.

The minimum annual streamflow occurred in 1997 at all stations except for Tangnaihai where the minimal streamflow occurred in 2002 (Figure 3A–G). At all stations, the six-year running streamflow from 1997–2002 was the lowest for the 60-year period (1957–2016). Streamflow in rivers, e.g., the Mississippi [33], the Yangtze [34] and the Pearl River [35], normally increases downstream from the headwater to the river mouth. However, abnormal downstream decreases in streamflow were found in two reaches in the YR (i.e., the 1400 km reach between Lanzhou and Toudaoguai and the 800 km reach between Huayuankou and Lijin). For example, in 2016, the streamflow decreased from 26.8 km³/yr at Lanzhou to 14.4 km³/yr at Toudaoguai, and decreased from 20.6 km³/yr at Huayuankou to 6.98 km³/yr at Lijin (Figure 3H).

3.2. Climatic Impacts on the Temporal Trend in Streamflow

Despite the climate warming over the past decades, the potential evaporation both worldwide and in the YRB has shown a decreasing trend due to increased cloud cover and decreased wind speed [36,37]. A decrease in potential evaporation is more likely to have contributed to an increase rather than a decrease in streamflow. Thus, the streamflow decline in the YR could not be attributed to evaporation change. Precipitation has shown slight increasing trends in the headwaters and upper reaches (above Lanzhou) of the YR (Figure 3A,B; Table A2), suggesting that precipitation change was not responsible for the streamflow decline in the upstream reach of this river. However, the decreasing precipitation trends in the middle and lower reaches (Figure 3C–G) undoubtedly contributed to the streamflow decline. For the entire basin, the water from precipitation decreased by 7.1% from 359 km³/yr in 1957 to 334 km³/yr in 2016, based on the precipitation trend (Table A2). It is necessary to indicate that the temporal regression trends in precipitation mentioned above are all nonsignificant in statistics (Table A2), and that their applications are less reliable than significant trends if there are. Nevertheless, we suppose that the utilization of these nonsignificant trends is better than no trend and can be used in identifying the impact of precipitation change on streamflow. Prior to the 1970s, there was little revegetation in the YRB, as addressed below. Therefore, the impact of revegetation before 1970 was negligible. For the period prior to 1970, our reconstructed natural streamflow (Q_N) at Lijin (i.e., the sum of the measured streamflow, water consumption and water impoundment by reservoirs) was closely correlated with the basin-wide water from precipitation (P_W) ($Q_N = 0.181 P_W^{1.021}$, $R = 0.86$, $p < 0.01$). Based on this relationship, the precipitation decline from 1957 to 2016 led to a streamflow decrease of 5.3 km³/yr (11%), which explains 13% of the trend-based total streamflow decrease at Lijin (39.9 km³/yr) over the past 60 years (Figure 3G, Table A2).

In the same way, we can estimate the impact of decreased precipitation on streamflow at the stations between Lanzhou and Lijin. For example, at the Longmen Station (middle reach), the corresponding

correlation was $Q_N = 0.284 P_W^{0.925}$ ($R = 0.95$, $p < 0.0001$). The correlation equation predicts that the Q_N decreased from 39.3 km³/yr in 1957 to 38.1 km³/yr in 2016 as the P_W decreased from 206.6 km³/yr in 1957 to 199.8 km³/yr in 2016 (Figure 3D, Table A2). That is, the decreased precipitation between 1957 and 2016 alone has led to a decrease in streamflow measured at Longmen of 1.2 km³/yr (3.5%), which was 6.5% of the trend-based total streamflow decrease at Longmen (18.4 km³/yr) over the past 60 years (Figure 3D, Table A2).

The six-year running basin-wide precipitation from 1997–2002 was the lowest for the 60-year period, which agreed well with the minimum six-year running streamflow at Lijin. Thus, the extraordinary drop in streamflow from 1997–2002 was mainly owing to precipitation decline. The average basin-wide water from precipitation increased from 309 km³/yr from 1997–2002 to 350 km³/yr from 2003–2016. Based on the above correlation between Q_N and P_W , the Q_N increased by 8.6 km³/yr from 1997–2002 to 2003–2016. The average streamflow measured at Lijin increased by 12.3 km³/yr from 5.5 km³/yr in 1997–2002 to 17.8 km³/yr in 2003–2016. Approximately 70% of the streamflow increase from 1997–2002 to 2003–2016 was attributable to increased precipitation. In other words, the dominant cause of the streamflow resilience since 2003 was precipitation recovery, which disproved previous arguments that the streamflow resilience after the severe decline from 1997–2002 was owing to water regulation [17]. The conclusion that ‘since 2000, government management schemes have prevented streamflow from declining further and guarantee its stability [17] is debatable, because the authors neglected the important impact of precipitation increase on the YR streamflow since 2000. In their study, natural water yield is defined as the sum of streamflow, human water consumption and reservoir water storage change [17]. In fact, natural water yield mainly depends on precipitation. Since 2000, both water consumption (Figure 4D) and area of revegetation [21] have increased, which would have reduced the streamflow, if the precipitation had not increased. We argue that water regulation schemes (mainly via adjustment of reservoir operation) can change the distribution of streamflow between days, seasons and years, but they cannot reverse the long-term streamflow trend. In short, without precipitation recovery, there would have been no streamflow resilience in recent years.

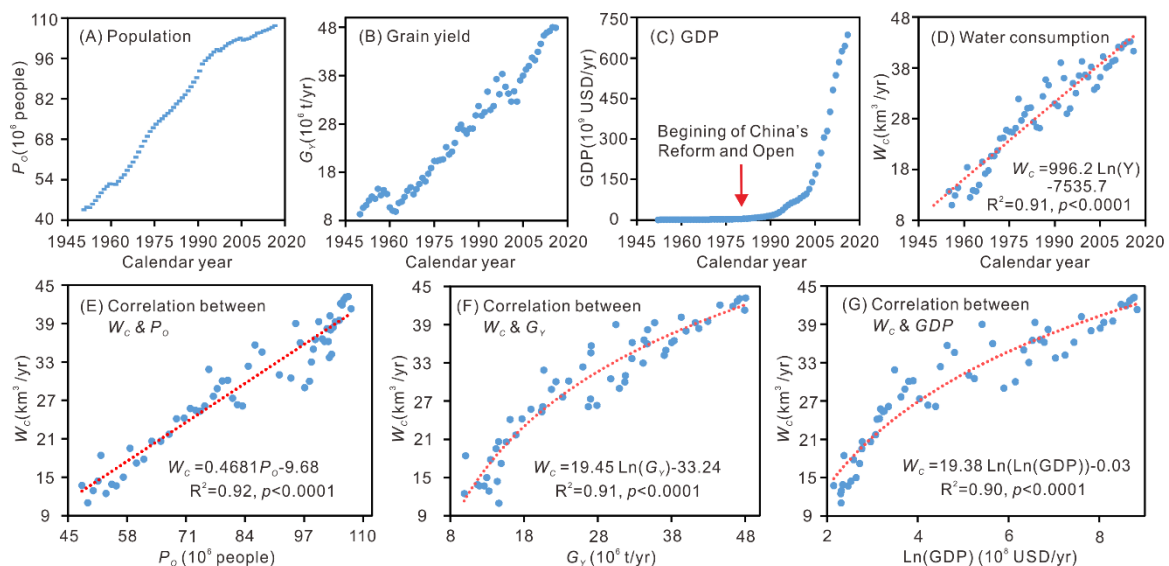


Figure 4. Rapid increases in population (P_o), grain yield (G_y), gross domestic product (GDP) and water consumption (W_c), and the close correlations with between W_c and P_o , G_y and GDP within the Yellow River basin. Y: Calendar year. R: Correlation coefficient. p: Significance level.

3.3. Human Impacts on the Temporal Trend in Streamflow

3.3.1. Water Consumption

The water consumption in the YRB has rapidly increased with socioeconomic growth over the past decades, and the increasing trend in water consumption was highly statistically significant ($R = 0.95$, $p < 0.0001$) (Figure 4). Based on the regression trend (Figure 4D), basin-wide water consumption increased by $30.4 \text{ km}^3/\text{yr}$ from 1957 ($14.3 \text{ km}^3/\text{yr}$) to 2016 ($44.7 \text{ km}^3/\text{yr}$), which can explain 76% of the total streamflow loss at Lijin from 1957–2016, even though its impact on streamflow varied among years (Figure 5). This water consumption was mainly attributable to agriculture, although industry and urbanization are becoming increasingly important. On average, 86%, 11% and 3% of the water consumption were due to agriculture, industry and urbanization, respectively. The weight of industry and urbanization in water consumption increased by half (from 10% to 15%) over the past two decades (Table A3). Spatially, approximately 40% of the water consumption occurred in the upper reaches (above the Toudaoguai Station), 30% in the middle reaches (between the Toudaoguai and Huayuankou Stations) and 30% in the lower reaches (below the Huayuankou Station) (Table A3).

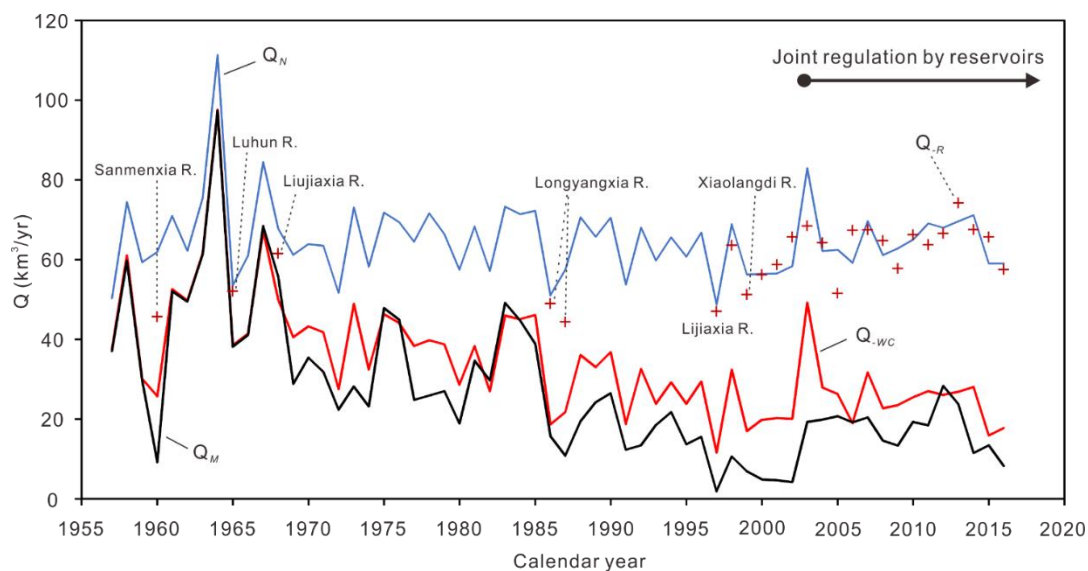


Figure 5. Human impacts on annual streamflow (Q) to the sea in the Yellow River. Q_N : Natural Q derived from precipitation (without human impact). Q_R : Q_N deduced by the impact of a reservoir or reservoirs. Q_{WC} : Q_N deduced by water consumption. Q_M : Streamflow measured at Lijin Station (with human impacts). The difference between Q_N and Q_M reflects the total impact of human activities. Sanmenxia R., Luhun R., Liujiaxia R., Longyangxia R., Lijiaxia R. and Xiaolangdi R. indicate that the major reservoirs each reduced the streamflow by $>1 \text{ km}^3$ at the initial water impoundment. Detailed information on these reservoirs is shown in Figure 1A and Table A4.

Considering that irrigation in the YRB has a long history, the streamflow must have been reduced by agriculture for a long time. Water diversion for irrigation from the YR began 2000 years ago, and the irrigation area was approximately $10,000 \text{ km}^2$ from 1522–1566 and $13,000 \text{ km}^2$ in 1937 (Figure 6). The irrigation area increased to 14,000, 20,000, 33,000, 41,000 and $48,000 \text{ km}^2$, respectively, in the 1950s, 1960s, 1970s, 1980s and from 1990–1995 (Figure 6). The population in the YRB was 48×10^6 , 57×10^6 , 72×10^6 , 83×10^6 and 95×10^6 people, respectively, in the 1950s, 1960s, 1970s, 1980s and from 1990–1995 (Figure 4A). The irrigation area was closely correlated with the population in the five most recent periods ($R^2 = 0.99$, $p < 0.0001$). Based on the regression equation between irrigation area and population, the irrigation area would have reached $57 \times 10^3 \text{ km}^2$ by 2016 (Figure 6) when the population was 107×10^6 people. We assumed that the irrigation area at the beginning stage in 2000 BP (years before present) was very small. Then we can conclude that the irrigation area in the

YRB slowly increased from near zero in 2000 BP to 14,000 km² in the 1950s and then rapidly increased to nearly 60,000 km² at present. Correspondingly, the water consumption likely increased slowly from zero in 2000 BP to 13 km³/yr in the 1950s, and afterwards rapidly increased to 45 km³/yr in 2016. Our results suggest that the history of human impacts on streamflow in this river was much longer than reported in previous studies that supposed the streamflow in the YR began to decrease in the 1970s due to precipitation decline and human impacts [20,21]. By the 1950s, water consumption may have reduced the streamflow by ~20%.

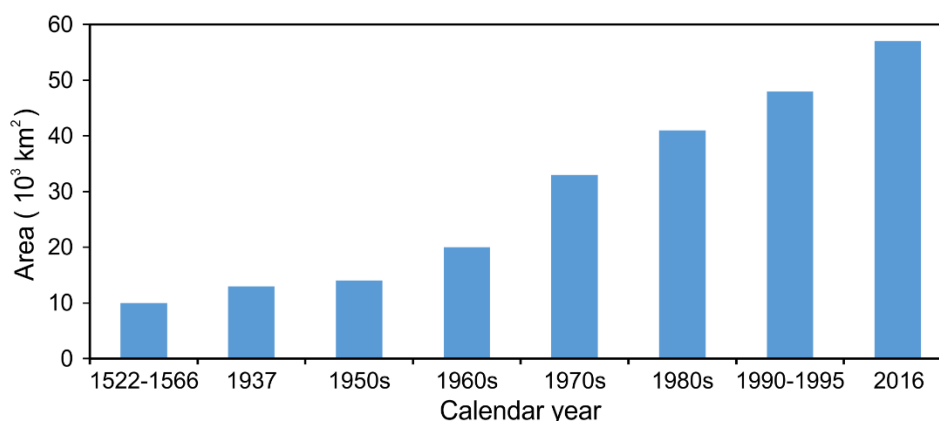


Figure 6. Historical increase in irrigation area within the Yellow River Basin (the data in 1522–1566 and 1937 are after Lu [38]; the data in the 1950s, 1960s, 1970s, 1980s and 1990–1995 are after Miao et al. [21])

Over the past decades, approximately 80% of the water consumption was derived from surface water and ~20% from groundwater. We assume that most of the groundwater extraction has been balanced by surface water infiltration, because a lower groundwater level tends to strengthen surface water infiltration and the groundwater in the YRB has a renewable nature. For example, the annual groundwater reserves in the YRB was 35.2 km³ in 2004 and 35.5 km³ in 2016, and there was no significant changing trend in the groundwater reserves between 2004 and 2007 ($R^2 = 0.002$, $p = 0.85$), based on data issued by the Ministry of Water Resources of China [39]. Thus, the total water consumption data can reflect the impact of water usage on streamflow.

3.3.2. Reservoir Construction

More than 3000 reservoirs have been constructed in the YRB since the 1950s [40]. In 2016, the total water storage in reservoirs in the YRB was 35 km³, 26 km³ of which was stored in seven of the major reservoirs, i.e., Longyangxia, Liujiaxia, Wanjiatai, Sanmenxia, Xiaolangdi, Luhun and Guxian [41]. The total maximum storage capacity of the seven major reservoirs was 66 km³ (Table A4). That the actual water storage in the seven major reservoirs (26 km³) was much smaller than their total maximum storage capacity (66 km³) may be partly due to reservoir sedimentation. For eight of the major reservoirs in the YRB, both maximum storage capacity and surface area were available. The total maximum storage capacity and surface area of the eight major reservoirs were 67.6 km³ and 1202 km², respectively (Table A4). Assuming that surface area is proportional to storage capacity, we estimated that the total surface area of reservoirs in the YRB in 2016 is approximately 1600 km². Considering that the potential evaporation within the YRB basin is 1690 mm/yr on average, the water surface evaporation from the reservoirs would be ca. 2.7 km³/yr, or 1.35 km³/yr larger than the evapotranspiration under primary non-reservoir conditions [14,29]. That is, reservoirs in the YRB together increased evaporation by 1.35 km³/yr, which can explain 3.5% of the decreased streamflow at Lijin from 1957 to 2016.

Based on the decreasing streamflow trend from 1957 to 2016 (Table A2), the cumulative loss of streamflow at Lijin over the past six decades was approximately 1200 km³. Nearly 3% of this cumulative streamflow loss can be attributed to the net water storage in reservoirs as observed in

2016 (35 km^3). The net water storage was the combined effect of water impoundment by all reservoirs. The water impoundment events in reservoirs were randomly distributed over the past six decades (Table A4). Water impoundments by reservoirs significantly reduced the water discharge to the sea in some individual years (Figure 5). In comparison, their combined effect accounted for less of the decreasing streamflow trend from 1957 to 2016. However, it is unreasonable to assume that water impoundments by reservoirs during the past decades was completely irrelevant to the streamflow decline. For example, net reservoir water impoundment in the YRB showed an increasing trend (Table A3). Without the changes in net reservoir water impoundment (Table A3), the decreasing rate of linear trend in streamflow at Lijin from 1957 to 2016 would be $0.6617 \text{ km}^3/\text{yr}$, or $0.0144 \text{ km}^3/\text{yr}$ lower than the decreasing rate of linear trend in streamflow measured at Lijin from 1957 to 2016 ($0.6761 \text{ km}^3/\text{yr}$, Table A2). That is, the increasing trend in net reservoir water impoundment resulted in a cumulative streamflow reduction by 0.86 km^3 over the past 60 years, which was responsible for 2.2% of the trend-based cumulative decrease in streamflow at Lijin from 1957 to 2016 ($39 \text{ km}^3/\text{yr}$). Considering that the reservoir-increased evaporation in the YRB was responsible for 3.5% of the trend-based cumulative decrease in streamflow at Lijin from 1957 to 2016, we roughly estimate that reservoir-increased evaporation and water impoundment together explain approximately 6% of the decreased streamflow at Lijin from 1957 to 2016. The water regulation by reservoirs since 2002, which modulated the streamflow distribution between years (Figure 5), months and days, has contributed to maintaining an inviolable flow throughout the hydrological year [42]. However, this water regulation by reservoirs has unlikely changed the long-term streamflow trend and was not a factor either slowing or speeding up the streamflow decline in the YR over the past six decades.

3.3.3. Revegetation

The area of afforestation and grass planting (AGP) for the purpose of water and soil conservation in the YRB increased from 8000 km^2 in 1959 to $12,000 \text{ km}^2$ in 1969, $31,000 \text{ km}^2$ in 1979, $95,000 \text{ km}^2$ in 1989 and $170,000 \text{ km}^2$ (23% of the catchment area) by the 2010s, which effectively improved plant productivity, expanded vegetation cover and increased transpiration, and thereby reduced the streamflow [21,43–45]. However, the processes and underlying mechanisms between revegetation and streamflow decline are complicated, and the area where these processes occurred is very large. For these reasons, it is currently difficult to directly quantify the basin-wide AGP impact on streamflow [44]. Because the potential evaporation in the YRB has not shown any increasing trend over the past decades [36], evaporation change is unlikely to be responsible for the streamflow decline at Lijin. Considering that water consumption, precipitation decrease and reservoir construction contributed to 76%, 13% and 6% of the streamflow decline at Lijin, respectively, we attribute the remaining 5% of the decreased streamflow at Lijin mainly to APG.

3.3.4. Land Use/Cover Change

In many previous studies, the streamflow decline in the YRB was simply attributed to land use/cover changes and climatic changes [46–48]. Thus, land use/cover change is a byword for human activities as one of the two causes of the streamflow decline in the YRB. Of course, land use/cover change is a major cause of the streamflow decline in the YRB. For example, the cultivated land area in China increased by 21% from $1,120,000 \text{ km}^2$ in 1957 [49] to $1,350,000 \text{ km}^2$ in 2016 [50]. Although the temporal trend in cultivated land area in the YRB during the same period is unavailable, we assume that it is similar to the countrywide temporal trend, because the YRB is an important component of China's breadbasket. The threefold increase in grain yield in the YRB from 1957 to 2016 (Figure 4B) should be attributed to both an increase in yield per unit area and an increase in cultivate land area. As the causes of the streamflow decline in the YRB, the reservoir construction and revegetation both can be treated as land use/cover changes. However, it would be unwise to attribute all human-induced streamflow decline to land use/cover changes. As shown above, water consuming increase has been the principal cause of the streamflow decline in the YR. The industry water consuming and urban water consuming

have increased more rapidly than the agriculture water consuming (Table A3), and the increase in agriculture water consuming has been partly attributable to the increase in grain yield per unit area. It is not proper to attribute the streamflow decline due to industry development, urbanization and increased grain yield per unit area to land use/cover change. The causes of the streamflow decline in the YR can be categorized into three subsets: water use/consuming, climatic change and land use/cover change [51]. In this study, we attributed streamflow decline in the YR mainly to four driving factors: increased water consuming, decreased precipitation, construction and operation of new reservoirs and revegetation.

3.4. Temporal Variation in the Weights of Factors Affecting Streamflow

Our results of the weights of factors in streamflow decline are largely different from earlier studies. Decrease precipitation was previously reported to be the main cause (75%–57%) of streamflow decline in the upper reaches (above Lanzhou) and middle reaches of the YR [14] and as important a cause as human activities (51% vs. 49%) for the decline in streamflow to the sea [18]. However, we found that the precipitation in the upper reaches of this river has shown an increasing trend over the past six decades (Figure 3A–B, Table A2), which presumably was not responsible for the streamflow decline. We also found that the decrease in basin-averaged precipitation can explain only 13% of the decreased streamflow to the sea. In the middle reaches, less than 10% of the streamflow decline can be attributed to decreased precipitation. Our disagreement with previous studies can be mainly attributed to the temporal variability of factors influencing streamflow. The data series in previous studies covered the periods from 1956–2000 [14] or 1950–2000 [18]. During these studied periods, precipitation showed a decreasing trend all over the YRB [14,18], and water consumption (the major cause of streamflow decline) was significantly less than in the present time (Figure 4D). Both precipitation and water consumption in the YRB have significantly increased in the most recent 1.5 decades (Figure 3A–G), which would decrease the weight of precipitation change and increase the weight of human impact in causing the streamflow decline. This finding demonstrates that the relative importance of climatic and anthropogenic impacts on streamflow can vary greatly over time.

3.5. Natural and Socioeconomic Causes of Severer Streamflow Decline in Downstream Areas

Although previous studies have found that the decline in streamflow in the YR was aggravated downstream of the upper reaches [21,52], less is known about the underlying causes. Here, we show that, from the headwaters to the lower reaches, the 60-year average population density, grain yield per unit area and gross domestic product (GDP) per unit area increased by more than two orders of magnitude (Figure 7A–C; Table A5). The rapid downstream increases in population density and grain yield per unit area are closely correlated (Figure 7F), which reflects that the areas with high population density are also the areas with high grain yield. Subsequently, the water consumption per unit area increased by more than two orders of magnitude from the headwaters to the lower reaches (Figure 7E; Table A5). The per capita precipitation water resources decreased by two orders of magnitude (Figure 7D; Table A5). These results suggest that the conflict between water availability and water demand was more serious in the lower reaches than in the upper reaches. As a result, the human impact on streamflow increased downstream. Additionally, the growths of population density, grain yield per unit area and GDP per unit area over the past 60 years have increased downstream. From the period 1957–1966 to the period 2007–2016, the population density growth increased from 2 p/km² in the headwater areas to 270 p/km² in the lower reaches, the growth of grain yield per unit area increased from 0.6 t/km² in the headwater areas to 240 t/km² in the lower reaches, and the growth of GDP per unit area increased from 22,000 USD/km² in the headwater areas to 3,600,000 USD/km² in the lower reaches (Table A5).

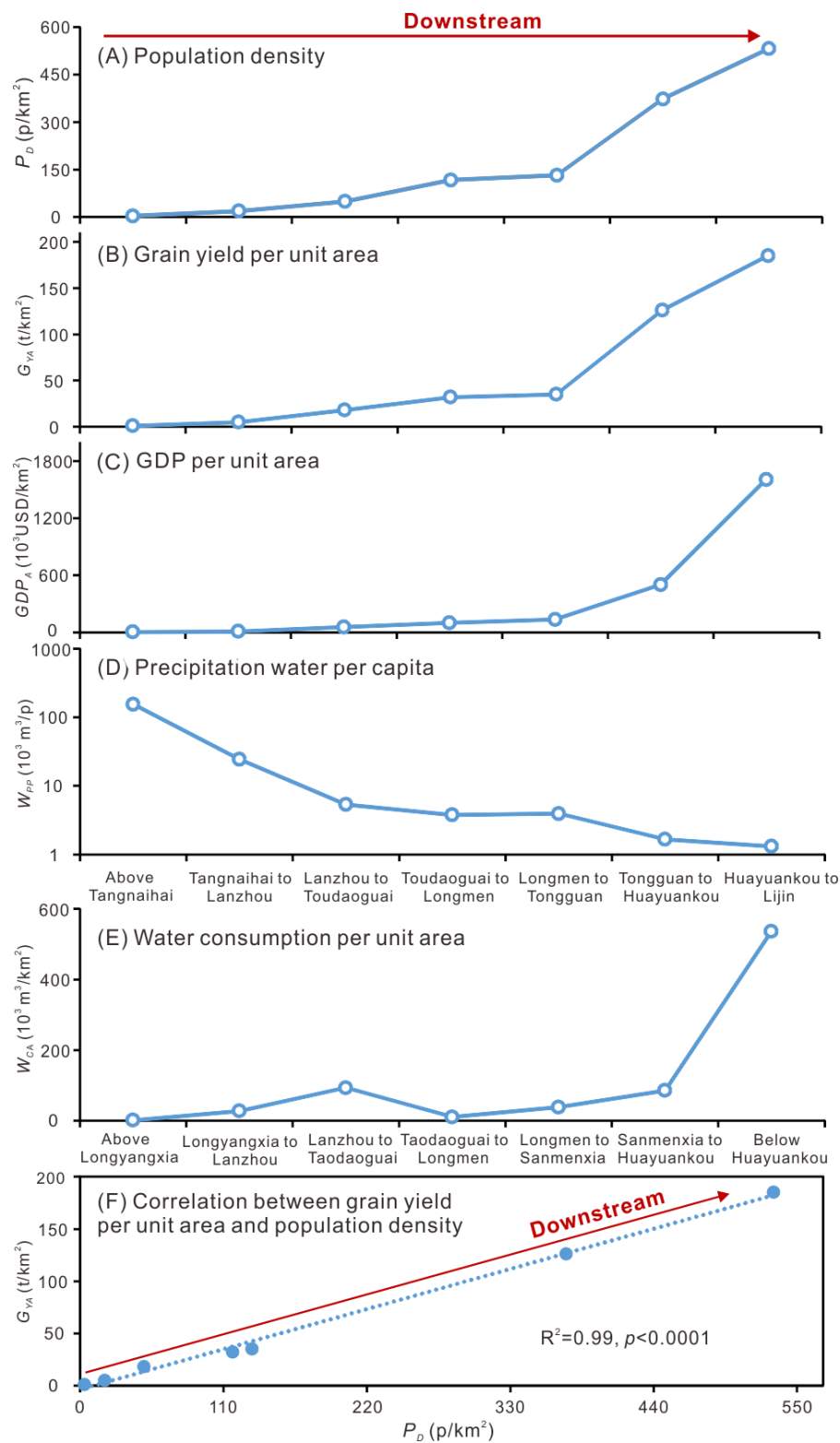


Figure 7. Rapid downstream changing trends in socioeconomic factors and water availability/consumption and close correlation between population density and grain yield per unit area along the Yellow River. P_D : Population density. G_{YA} : Annual grain yield per unit area. GDP_A : Annual GDP per unit area. W_{PP} : Annual precipitation water per capita. W_{CA} : Annual water consumption per unit area. All data are multi-year averages (see Table A5 for details).

The rapid downstream increases in population density, grain yield per unit area and GDP per unit area can be primarily attributed to the general downstream decrease in elevation and topographical relief and the downstream increase in temperature. The land elevation decreases from >5000 m in the headwaters to less than 500 m in the lower reaches, and the long-term annual average temperature increases from $-2\text{ }^{\circ}\text{C}$ in the headwaters to $12\text{ }^{\circ}\text{C}$ in the lower reaches (Figure 1). That is, the natural conditions become more suitable for agriculture and human development downstream, and agriculture and human development are the primary causes of downstream intensified water consumption and streamflow decline. According to the temporal trends in precipitation, from 1957 to 2016, the precipitation-water changes were +2.6% at Tangnaihai, +2.1% at Lanzhou, -1.0% at Toudaoguai, -3.3% at Longmen, -6.7% at Tongguan, -7.0% at Huayuankou and -7.1% at Lijin (Figure 3; Table A2). These results suggest that precipitation change may have also contributed to the downstream intensified decline in streamflow. In addition to the above influences, the unique downstream decrease in streamflow between Lanzhou and Toudaoguai (Figure 3H) may also be attributable to the extremely low amount of water provided by precipitation per unit area (Figure 1C; Table A6), the extremely high potential evaporation (Figure 1D) and the high amount of water consumption per unit area in this region (Figure 1C; Table A6).

3.6. Trend-Based Predictions of Future Streamflow

Over the past six decades, the streamflow trend in the YR was determined mainly by precipitation change and socioeconomic development. Similar to past decades, precipitation change and socioeconomic development can be expected to be dominant factors influencing the future streamflow trend in the YR. Therefore, understanding future trends in precipitation and socioeconomic development are the most important for predicting the future streamflow in this river.

Although it has been predicted that the global precipitation will increase in the long term with global warming at a rate of 1% to $3\%/^{\circ}\text{C}$, the local precipitation responses will be heterogeneous [53]. In fact, the precipitation within the YRB has shown a slight decreasing trend (-5.6 mm/decade) since the 1950s (Figure 3G), even though the global temperature ($0.21\text{ }^{\circ}\text{C/decade}$) and the temperature in the YRB ($0.27\text{ }^{\circ}\text{C/decade}$) have shown a rapid increasing trend during the same period [54]. It is highly uncertain whether precipitation trends in the YRB in future decades will be increasing or decreasing; however, it is believed that the trend will be small (a few percent at the century-scale) [9]. Thus, we predict the future streamflow in the YR under three precipitation trend scenarios: (1) the same trend as in the past six decades; (2) no increasing or decreasing trend; (3) an inverse trend to the past but with the same absolute change rate as the past trend.

China has an ambitious goal to construct a “modern powerful country” by the middle of this century [26]. Continued socioeconomic development will increase water consumption. Although the population growth rate in the YRB has slowed in the last 20 years (Figure 4A), as a result of China’s “one-child-per-couple” policy, the population will most likely rebound in the coming decades because of the recently issued “two-children-per-couple” policy. If the population in the YRB increases following the general trend of the past decades ($R^2 = 0.97$, $p < 0.0001$), it will reach 130 million by 2030. At this population level, the water consumption in the YRB ($51.2\text{ km}^3/\text{yr}$, based on the correlation in Figure 4E) would be $6.9\text{ km}^3/\text{yr}$ higher than the trend-based water consumption in 2016 ($44.3\text{ km}^3/\text{yr}$, based on the trend equation in Figure 4D), which approaches the trend-based streamflow at Lijin in 2016 ($6.98\text{ km}^3/\text{yr}$, based on the trend equation in Table A2). In addition, many reservoirs are under construction or in construction planning [55], and new projects for water and soil conservation will be implemented in the YRB [56]. Presumably, these programs will lead to a further decrease in streamflow in the YR. By 2030, the streamflow in the lower reaches of the YR will most likely be insufficient to satisfy the water requirements. For predicting the future streamflow in the YR, we can rationally assume that future socioeconomic growth will maintain the same rate as in past decades until it is slowed by water shortage.

In predicting the future streamflow in the YR, we employed the logarithmic equations (Table A2) for the following reasons. (1) The correlation coefficient of the logarithmic equation is the highest among the four regressions at Lijin Station (tidal limit) and close to the correlation coefficients of the linear, power and exponential regressions at other stations. (2) The logarithmic trend is assumedly better than the linear trend in predicting the future streamflow, because water shortage may probably slow socioeconomic growth and decrease the increasing rate of water consumption. (3) The logarithmic trend is assumedly better than the power and exponential trends, because the power trend-based and exponential trend-based predictions of the commence year for annual streamflow depletion are infinite, which is unrealistic. We assume that the annual streamflow in the lower YR will be depleted sooner or later, like the streamflow depletion that previously occurred in the lower reaches of the Nile and Colorado rivers [57–59]. We found that, if one makes the simplistic assumption that the past logarithmic trends in streamflow (Figure 3, Table A2) will continue, the streamflow will decrease to zero by 2029 at Lijin Station, 2063 at Huayuankou Station, 2063 at Tongguan Station, 2069 at Longmen Station, 2086 at Toudaoguai Station, 2215 at Lanzhou Station and 2385 at Tangnaihai Station (Table A2).

The past streamflow trends include the impacts of the precipitation changes, and therefore, cannot be directly employed for predicting the future streamflow trend, because we assumed that no changing trend in precipitation should be considered in predicting the future trend. To remove the influences of the past precipitation trends on streamflow, we modified the streamflow trend equation by adding precipitation trend-predicted water loss to the streamflow (see Methods for details). Then, we revised the prediction of the year when the annual streamflow will first be depleted to be 2031 at Lijin, 2068 at Huayuankou and Tongguan, 2074 at Longmen, 2091 at Toudaoguai, 2219 at Lanzhou and 2414 at Tangnaihai (Table A2). In a similar way, we predicted the year when the streamflow will be depleted for a scenario of an inverse precipitation trend but with an equal absolute change rate to that of the past six decades. Then, our predictions for the year when the annual streamflow will first be depleted and when year-round dry-up in the river will first occur can be expressed as 2031 ± 2 at Lijin, 2068 ± 9 at Huayuankou, 2068 ± 8 at Tongguan, 2074 ± 5 at Longmen, 2091 ± 6 at Toudaoguai, 2219 ± 13 at Lanzhou and 2414 ± 52 at Tangnaihai. Each number preceding “ \pm ” indicates the year when the annual streamflow will first be depleted under the scenario that no precipitation trend will be found in the future period. Each number following “ \pm ” indicates the years more/less than that preceding “ \pm ” needed for the scenario of increasing/decreasing precipitation trend. Similarly, if one makes the simplistic assumption that the past logarithmic trends in streamflow will continue, the streamflow will decrease to below 5% of its initial level by 2029 ± 2 at Lijin, 2063 ± 9 at Huayuankou, 2063 ± 8 at Tongguan, 2069 ± 5 at Longmen, 2086 ± 6 at Toudaoguai, 2215 ± 13 at Lanzhou and 2385 ± 52 at Tangnaihai.

There is uncertainty regarding the above predictions. First, we could not consider all the factors influencing the streamflow. For example, we did not include the impact of potential evaporation change on streamflow because of the complexity and uncertainty of its future trends [29,60]. Second, the future trends in precipitation and socioeconomic growth may probably deviate from our assumed trends, because the factors influencing them are complicated. Third, interannual variability of precipitation is high (Figure 3). The time of streamflow depletion would be earlier for low annual precipitation or later for high annual precipitation than we predicted. Thus, our predictions are only applicable to the precipitation and socioeconomic development scenarios we assumed.

However, the natural scenarios we assumed (or similar ones) will most likely occur in future decades. Our predictions show early warning signs of streamflow depletion in the YR. Most strikingly, streamflow depletion will probably begin to occur in the lower YR in late 2020s or early 2030s, unless effective countermeasures against water shortage are taken. The countermeasures could include (1) improving the efficiency of water usage especially in agriculture, (2) water diversion (e.g., 5–10 km³/yr) from the neighboring Yangtze River where water resources are relatively abundant [34] and (3) artificially increasing precipitation within the YRB [61]. These countermeasures rely on technological innovations and a large amount of capital investment. For example, assuming

a future scenario of a 10% increase in efficiency of water usage, the commence year of streamflow depletion at Lijin Station would be postponed by ca. 8 years. If the efficiency of water usage is increased by 20%, the commence year of streamflow depletion at Lijin Station would be postponed by ca. 18 years.

3.7. Consequences of Streamflow Decline

3.7.1. Ecosystem Degeneration

Streamflow decline tends to decrease the land–sea delivery of nutrients and sediment, resulting in ecosystem degeneration in estuaries, deltas and adjacent seas [62–64]. Extreme examples are found in the Nile and Colorado River systems, where streamflow depletions caused severe delta erosion and habitat loss for indigenous species, which led to a decline in fisheries [57–59]. Streamflow dry-up can be expected to cut off fish migration between upstream areas and the sea [65]. The amount of sediment discharge in the YR was once the largest in the world [6]. However, the sediment discharge from the YR to the Bohai Sea has decreased by more than 90% over the past decades due to streamflow decline and a reduction in suspended sediment concentration [66]. The dramatic decrease in sediment discharge has led to an imbalance between fluvial sediment supply and sediment dispersal under the hydrodynamic regime in coastal waters, thereby triggering delta erosion and coastal wetland degradation [67–69]. Despite the human-induced increase in nutrient concentration, the nutrient flux of the YR has decreased because of the dramatic streamflow decline [70]. Consequently, ecosystem degeneration, primary productivity reduction and a decline in fisheries in the YR estuary and adjacent waters have been observed [69]. A year-round streamflow dry-up below Lijin beginning in the late 2020s, as predicted above, would stop the delivery of fresh water, sediment and nutrients to the Bohai Sea and presumably would aggravate ecosystem deterioration in the estuary, delta and adjacent sea.

3.7.2. Socioeconomic Impacts

The close relationships between water consumption and population, grain yield and GDP (Figure 4) suggest that water shortages due to streamflow decline and dry-up will be an important constraint on sustainable socioeconomic development in the YRB as well as in other semi-arid areas in North China and the world. The major consequences could include deficiencies in domestic water use, decreases in irrigation area and grain yield, factory shutdowns and loss of shipping business. In fact, temporary dry-up events in the YR in 309 AD, 1372 AD and 1640 AD once brought about serious famines, considerable displacement of people and even reports of cannibalism [24]. Between 1972 and 1997, when the precipitation was lower than usual, seasonal dry-ups frequently occurred in the lower YR, with the greatest dry-up distance of 724 km and the longest dry-up duration of 226 days [22,71]. There are 10 large cities (each >0.5 million in population) along the dried-up reaches, including the provincial capitals of Zhengzhou and Jinan (both >2 million in population) (Figure 1A). These dry-ups led to a grain yield decrease of 0.7–0.8 Mt/yr and a direct GDP loss of 0.1 billion USD/yr, on average, in the entirety of 1972–1997 [25]. In the 1990s, the GDP loss caused by the dry-ups increased to 0.4 billion USD/yr [24]. The temporary dry-up events in the YR reflect the conflicts between the seasonal variability of water demand (especially in agriculture) and the distribution of water resources with the year, which should be considered in water management. No seasonal dry-up has occurred since 1998, because of joint water regulation by reservoirs [42] (Figure 6) and precipitation recovery (Figure 3). If year-round stream dry-ups truly occur in the YR, as predicted above, their socioeconomic impacts would be much more serious.

4. Conclusions

Over the past 60 years (1957–2016), streamflow decline was found in most reaches of the semiarid Yellow River. The decline was aggravated downstream from −14% at Tangnaihai (headwater reach) to −81% At Lijin (tidal limit). The streamflow decline was mainly (87%) attributed to rapid socioeconomic

development, which significantly increased water retention and water consumption within the drainage basin, although precipitation decrease was also responsible for this (13%). If the socioeconomic development in this basin keeps a growth rate equal to the past, year-round dry-up in the lower Yellow River may probably commence in the late 2020s or early 2030s, unless effective countermeasures are taken. Considering the high interannual variability of precipitation and streamflow, river dry-up may be intermittent in the early stage. In other words, annual streamflow depletion will occur first in drought years, then extend to normal and ultimately to wet years. If wet and dry years alternate, reservoirs can detain part of the streamflow in the wet year and release the detained water in the following dry year, thereby reducing the possibility of streamflow depletion in the dry year. The adjustable net storage capacity of the reservoirs in the YRB is currently $\sim 40 \text{ km}^3$, which is the same in magnitude of the long-term average of annual streamflow from the YR to the sea. However, when several dry years occur consecutively after the 2020s, year-round dry-up in the lower YR will probably be inevitable. Our results suggest that streamflow in semiarid basins is highly vulnerable to human impacts and that streamflow decline would in turn hinder further socioeconomic development and also endanger river-sea ecosystems. We appeal for in-depth studies on future streamflow trends under human and climatic impacts and for river-sea integrated and socioeconomic-ecosystem integrated water resources management within semiarid basins in North China and worldwide.

Author Contributions: Conceptualization, X.L. and H.Y.; Data curation, Q.T.; Formal analysis, X.L., H.Y. and S.C.; Funding acquisition, S.L.Y.; Investigation, J.F. and S.Z.; Methodology, B.S.; Project administration, B.S.; Resources, Q.T. and Y.Z.; Software, S.C.; Validation, Y.Z. and H.W.; Visualization, X.S.; Writing—original draft, S.L.Y. All authors have read and agreed to the published version of the manuscript.

Acknowledgments: This work was supported by the Ministry of Science and Technology of China (2016YFA0600901, 2016YFE0133700) and the Natural Science Foundation of China (U1606401; U1706214).

Conflicts of Interest: The authors declare no conflict of interest.

Appendix A

Table A1. Natural and socioeconomic factors influencing streamflow in the Yellow River Basin in comparison with global factors.

Variables	Yellow River Basin	Data Sources (Reference)	Global Total/Average	Data Sources (Reference)
Catchment area (10^3 km^2)	752	(38)	105,000	(6)
Range of latitude ($^{\circ}\text{N}$)	32.2–41.8	(53)	–	
Temperature ($^{\circ}\text{C}$) ^a	7.0	This study (calculation)	–	
Precipitation (mm) ^a	459	This study (calculation)	953	[72]
Pan evaporation (mm) ^a	1690	(35)	1150	[73]
Runoff (km^3/yr) ^{a,b}	65	This study (calculation)	39,000	[74]
Population (10^6 people) ^c	107	This study (calculation)	7400	https://www.baidu.com
Population density (people/ km^2) ^c	142	This study (calculation)	70	This study (calculation)
Total precipitation water (km^3/yr) ^a	345	This study (calculation)	100,000	This study (calculation)
Precipitation water per capita ($10^3 \text{ m}^3/\text{person}/\text{yr}$) ^a	3.22	This study (calculation)	13.5	This study (calculation)
Runoff per capita ($10^3 \text{ m}^3/\text{person}/\text{yr}$) ^a	0.61	This study (calculation)	5.23	This study (calculation)
Grain yield ($10^6 \text{ t}/\text{yr}$) ^c	47.9	This study (calculation)	2880	https://www.baidu.com
Grain yield per unit area ($10^3 \text{ t}/\text{km}^2/\text{yr}$) ^c	63.4	This study (calculation)	2.74	This study (calculation)
Grain yield per capita (t/person/yr) ^c	0.45	This study (calculation)	0.39	This study (calculation)
Grain yield per unit runoff ($10^3 \text{ t}/\text{km}^3/\text{yr}$) ^c	737	This study (calculation)	73.8	This study (calculation)
GDP ($10^9 \text{ USD}/\text{yr}$) ^c	686	This study (calculation)	75,900	World Bank (https://data.worldbank.org.cn)
GDP per unit area ($10^3 \text{ USD}/\text{km}^2/\text{yr}$) ^c	912	This study (calculation)	542	This study (calculation)
GDP per capita ($10^3 \text{ USD}/\text{person}/\text{yr}$) ^c	6.4	This study (calculation)	10.3	This study (calculation)
GDP per unit runoff ($10^9 \text{ USD}/\text{km}^3/\text{yr}$) ^c	10.6	This study (calculation)	1.95	This study (calculation)

^a Regional and multi-year average. ^b Runoff means streamflow derived from precipitation (without human impact).

^c Present level (2016).

Table A2. Results of Mann–Kendall (MK) test and linear, logarithmic, power and exponential regresses for temporal trends (1957–2016) in annual precipitation and streamflow in the YRB, and trend-based prediction of calendar year when annual stream dry-up will commence.

Gauging Stations	P_W and Q_M	Z_{MK}	β	Trend Equation	R	p	Trend-Based Change from 1957 to 2016 (%) ^a	Trend-Based Prediction of Calendar Years for Commence of 5% Streamflow (and Depletion) ^b
Tangnaihai	P_W	0.61	−1.35	$P_W = 0.0236Y + 18.07$	0.058	0.66 (nonsignificant)	+2.2	
				$P_W = 47.10\ln(Y) + 272.7$	0.058	0.66 (nonsignificant)	+2.2	
				$P_W = 0.0999Y^{0.8521}$	0.068	0.52 (nonsignificant)	+2.6	
				$P_W = 27.64e^{0.0004Y}$	0.068	0.52 (nonsignificant)	+2.4	
	Q_M	0.04	−0.04	$Q_M = -0.0468Y + 112.9$	0.157	0.23 (nonsignificant)	−13 (−15)	2340 ± 50 (2360 ± 52)
				$Q_M = -92.57\ln(Y) + 723.0$	0.157	0.23 (nonsignificant)	−13 (−15)	2385 ± 53 (2414 ± 55)
				$Q_M = 8E+17Y^{-5.038}$	0.177	0.18 (nonsignificant)	−14 (−16)	3343 ± 205 (Infinite)
				$Q_M = 3028.6e^{-0.00255Y}$	0.178	0.18 (nonsignificant)	−14 (−16)	2963 ± 172 (Infinite)
Lanzhou	P_W	0.52	0.05	$P_W = 0.0297Y + 51.56$	0.046	0.73 (nonsignificant)	+1.6	
				$P_W = 58.893\ln(Y) - 336.7$	0.046	0.73 (nonsignificant)	+1.6	
				$P_W = 0.6007Y^{0.6861}$	0.059	0.58 (nonsignificant)	+2.1	
				$P_W = 55.399 e^{0.000345Y}$	0.059	0.58 (nonsignificant)	+2.1	
	Q_M	−2.16	−0.11	$Q_M = -0.1321Y + 293.1$	0.349	0.006 (significant)	−23 (−24)	2208 ± 13 (2221 ± 13)
				$Q_M = -262.6\ln(Y) + 2024.8$	0.349	0.006 (significant)	−23 (−24)	2215 ± 13 (2219 ± 13)
				$Q_M = 1.14E+28Y^{-8.058}$	0.343	0.006 (significant)	−21 (−22)	2670 ± 180 (Infinite)
				$Q_M = 94134e^{-0.00404Y}$	0.343	0.006 (significant)	−21 (−22)	2636 ± 176 (Infinite)
Toudaoguai	P_W	−0.13	−0.03	$P_W = -0.0243Y + 194.9$	0.025	0.85 (nonsignificant)	−1.0	
				$P_W = -48.44\ln(Y) + 514.5$	0.025	0.85 (nonsignificant)	−1.0	
				$P_W = 107.2 Y^{0.0404}$	0.003	0.94 (nonsignificant)	+0.1	
				$P_W = 139.88e^{2E-05Y}$	0.003	0.94 (nonsignificant)	+0.1	
	Q_M	−3.92	−0.18	$Q_M = -0.2130Y + 443.8$	0.494	<0.0001 (very significant)	−47 (−46)	2084 ± 6 (2089 ± 6)
				$Q_M = -423.1\ln(Y) + 3233.8$	0.494	<0.0001 (very significant)	−46 (−45)	2086 ± 6 (2091 ± 6)
				$Q_M = 5.6E+67Y^{-20.15}$	0.510	<0.0001 (very significant)	−45 (−44)	2312 ± 37 (Infinite)
				$Q_M = 8.3E+9e^{-0.01Y}$	0.510	<0.0001 (very significant)	−45 (−44)	2298 ± 37 (Infinite)
Longmen	P_W	−0.25	−0.05	$P_W = -0.1157Y + 433.0$	0.077	0.56 (nonsignificant)	−3.3	
				$P_W = -231.4\ln(Y) + 1960.5$	0.078	0.55 (nonsignificant)	−3.3	
				$P_W = 16609Y^{-0.581}$	0.040	0.77 (nonsignificant)	−1.7	
				$P_W = 357.9e^{-3E-04Y}$	0.039	0.79 (nonsignificant)	−1.8	
	Q_M	−5.17	−0.27	$Q_M = -0.3117Y + 644.1$	0.623	<0.0001 (very significant)	−54 (−51)	2067 ± 5 (2071 ± 5)
				$Q_M = -619.1\ln(Y) + 4726.8$	0.623	<0.0001 (very significant)	−53 (−50)	2069 ± 5 (2074 ± 5)
				$Q_M = 1.75E+82Y^{-24.52}$	0.651	<0.0001 (very significant)	−52 (−49)	2237 ± 36 (Infinite)
				$Q_M = 5.48E+11e^{-0.012Y}$	0.651	<0.0001 (very significant)	−51 (−48)	2243 ± 36 (Infinite)

Table A2. Cont.

Gauging Stations	P_W and Q_M	Z_{MK}	β	Trend Equation	R	p	Trend-Based Change from 1957 to 2016 (%) ^a	Trend-Based Prediction of Calendar Years for Commence of 5% Streamflow (and Depletion) ^b
Tongguan	P_W	−0.70	−0.21	$P_W = -0.3539Y + 1004$	0.159	0.23 (nonsignificant)	−6.7	
				$P_W = -705.2\ln(Y) + 5656.1$	0.159	0.23 (nonsignificant)	−6.7	
				$P_W = 5.8E+08Y^{-1.905}$	0.130	0.31(nonsignificant)	−5.5	
				$P_W = 1992.5e^{-1E-03Y}$	0.131	0.30(nonsignificant)	−5.5	
	Q_M	−5.53	−0.40	$Q_M = -0.4568Y + 940.0$	0.643	<0.0001 (very significant)	−59 (−50)	2061 ± 8 (2066 ± 8)
				$Q_M = -994.8\ln(Y) + 7590.1$	0.643	<0.0001 (very significant)	−58 (−50)	2063 ± 8 (2068 ± 8)
				$Q_M = 3.96E+93Y^{-27.93}$	0.678	<0.0001 (very significant)	−56 (−48)	2216 ± 35 (Infinite)
				$Q_M = 3.65E+13e^{-0.014Y}$	0.678	<0.0001 (very significant)	−56 (−48)	2208 ± 34 (Infinite)
Huayuankou	P_W	−0.71	−0.23	$P_W = -0.4101Y + 1146$	0.168	0.20 (nonsignificant)	−7.0	
				$P_W = -817\ln(Y) + 6535.7$	0.168	0.20 (nonsignificant)	−7.1	
				$P_W = 1.85E+09Y^{-2.045}$	0.143	0.28 (nonsignificant)	−5.9	
				$P_W = 2523.8e^{-0.00102Y}$	0.143	0.28 (nonsignificant)	−5.9	
	Q_M	−5.13	−0.43	$Q_M = -0.5007Y + 1030.0$	0.606	<0.0001 (very significant)	−59 (−50)	2061 ± 9 (2066 ± 9)
				$Q_M = -994.8\ln(Y) + 7590.1$	0.607	<0.0001 (very significant)	−59 (−50)	2063 ± 9 (2068 ± 9)
				$Q_M = 3.05E+91Y^{-27.29}$	0.621	<0.0001 (very significant)	−56 (−48)	2213 ± 33 (Infinite)
				$Q_M = 2.45E+13e^{-0.0138Y}$	0.621	<0.0001 (very significant)	−56 (−48)	2205 ± 32 (Infinite)
Lijin	P_W	−0.81	−0.26	$P_W = -0.4316Y + 1204$	0.171	0.19 (nonsignificant)	−7.1	
				$P_W = -859.9\ln(Y) + 6876.6$	0.171	0.19 (nonsignificant)	−7.1	
				$P_W = 2.35E+09Y^{-2.07}$	0.146	0.27 (nonsignificant)	−6.0	
				$P_W = 2705.7e^{-0.001Y}$	0.146	0.27 (nonsignificant)	−5.9	
	Q_M	−5.64	−0.61	$Q_M = -0.6761Y + 1370$	0.654	<0.0001 (very significant)	−85 (−74)	2026 ± 2 (2028 ± 2)
				$Q_M = -1344\ln(Y) + 10235.9$	0.656	<0.0001 (very significant)	−81 (−70)	2029 ± 2 (2031 ± 2)
				$Q_M = 3.35E+170Y^{-51.3}$	0.609	<0.0001 (very significant)	−78 (−68)	2075 ± 12 (Infinite)
				$Q_M = 4.1E+23e^{-0.026Y}$	0.608	<0.0001 (very significant)	−78 (−68)	2075 ± 12 (Infinite)

Z_{MK} : Significance level of MK test; $|Z_{MK}| > 1.96$ is defined to be significant in statistics; positive and negative Z_{MK} values indicate increasing and decreasing trends, respectively. β : Average change rate of MK test. P_W : Water from precipitation (km^3/yr). Q_M : Measured streamflow (km^3/yr). Y : Calendar year. R : Correlation coefficient of regression. p : Significance level of regression; $p < 0.05$ is defined as statistically significant [75,76].^a The streamflow change (%) outside of the brackets were directly predicted using the streamflow trend equation, whereas the value within the brackets were predicted using revised equations in which the influences of the precipitation changes on streamflow were excluded (for details, see the method section).

^b The number outside of the brackets indicates the prediction of year when streamflow will first decrease to below 5% of its initial level (i.e., the trend-based streamflow in 1957), whereas the number within the brackets were predicted for streamflow depletion. Each number preceding “±” indicates the calendar year predicted for the scenario that no precipitation trend will be found in the future period, whereas the number following “±” indicates the years more/less than that preceding “±” needed for the scenario of increasing/decreasing precipitation trend.

Table A3. Water extraction (W_E), water consumption (W_C), change in reservoir water impoundment (C_{WI}) and net reservoir water impoundment (N_{WI}) in the Yellow River Basin ^a

Periods	W_E (km ³)	W_C (km ³)	C_{WI} (km ³)	N_{WI} (km ³)	Spatial distribution of W_C (%)						Percentage of W_C (%)		
					Above LZ	LZ to TDG	TDG to LM	LM to SMX	SMX to HYK	Below HYK	Agriculture Use	Industry Use	Urban Use
1998	49.7	36.5	5.26	22.1	7	33	3	19	7	31	90	8	2
1999	51.7	39.3	4.96	27.0	7	34	2	19	7	32	90	8	2
2000	48.1	36.6	0.155	27.2	8	33	3	20	6	29	88	9	3
2001	47.5	36.2	−2.27	24.9	8	34	3	20	6	29	87	9	4
2002	49.5	38.2	−7.39	17.5	8	31	3	19	6	34	87	10	3
2003	42.9	33.7	14.41	31.9	6	31	4	20	8	31	86	12	2
2004	44.5	34.2	−2.18	29.7	9	35	3	20	7	26	87	11	2
2005	46.5	36.2	10.91	40.7	8	37	4	20	6	26	88	11	1
2006	51.2	40.2	−8.23	32.4	8	31	4	20	7	30	87	10	3
2007	48.5	38.0	2.15	34.6	8	32	4	21	7	27	87	11	2
2008	49.1	38.4	−3.68	30.9	8	32	4	20	8	29	86	12	2
2009	50.3	39.3	4.96	35.9	ND	ND	ND	ND	ND	ND	86	12	2
2010	51.2	39.5	−1.31	34.5	ND	ND	ND	ND	ND	ND	85	12	3
2011	53.6	42.1	5.3	39.8	ND	ND	ND	ND	ND	ND	85	13	2
2012	52.4	41.9	1.4	41.2	ND	ND	ND	ND	ND	ND	ND	ND	ND
2013	53.3	42.7	−4.63	36.6	11	30	4	19	7	29	85	12	3
2014	53.5	43.1	3.59	40.2	11	29	4	19	7	31	85	12	3
2015	53.5	43.2	−6.67	33.5	10	28	4	19	7	32	85	12	3
2016	51.5	41.3	1.47	35.0	11	28	4	20	7	30	85	12	3
Average	49.9	39.0	0.96	32.4	9	32	4	20	7	30	86	11	3

^a Data prior to 1998 are unavailable. LZ: Lanzhou; TDG: Toudaoguai; LM: Longmen; SMX: Sanmenxia; HYK: Huayuankou. ND: No data were available.

Table A4. Information on major reservoirs in the Yellow River Basin.

Name of Reservoir	Distance from Headwater (km)	Catchment Area (km ²)	Maximum Storage Capacity (km ³)	Regulating Storage Capacity (km ³)	Surface Area (km ²)	Time of Initial Water Impoundment
Longyangxia	1684	131,000	27.4 ^a	19.4	383	October 1986
Laxiwa	1716	ND	1.08 ^a	ND	ND	April 2009
Gongboxia	1754	ND	0.62 ^a	0.08	ND	September 2004
Liji Xia	1796	159,600	1.75 ^a	ND	32	December 1996
Jishixia	1900	ND	0.29 ^a	ND	ND	November 2010
Liujiaxia	2021	173,000	6.4 ^a	ND	130	October 1968
Yanguoxia	2026	183,000	0.22	ND	ND	November 1961
Daliushu	2346	252,000	11	5	ND	Construction in plan
Qingtongxia	2600	275,000	0.62	0.32	113	1968
Wanjiashai	3550	395,000	0.896 ^a	ND	ND	October 1998
Sanmenxia	4470	688,000	16.2	ND	200	January 1960
Xiaolangdi	4538	694,000	12.7 ^a	5.1	278	October 1999
Luhun	Tributary	3490	1.32 ^a	ND	31	1965
Guxian	Tributary	5370	1.2	ND	35	1994

Sources: ^a After Jia 2013 [77]. Other information is collected from <https://baike.so.com>. ND: No data were available.

Table A5. Downstream changes in natural and socio-economic factors in the Yellow River Basin.

Variables	Above TNH	TNH to LZ	LZ to TDG	TDG to LM	LM to TG	TG to HYK	HYK to LJ
Length of stream segment (km)	1553	543	1376	723	155	328	786
Catchment area (10 ³ km ²)	122	101	134	130	185	47.8	21.9
Precipitation water per unit area (10 ³ m ³ /p) ^a	543	464	262	442	521	623	702
Population density (p/km ²) ^a	3.5	19	49	117	132	373	532
Grain yield density (t/km ²) ^a	1	5	18	32	35	126	185
GDP per unit area (10 ³ USD/km ²) ^a	2.7	9.0	54	98	134	500	1606
Precipitation water per capita (10 ³ m ³ /p) ^a	155	24.4	5.35	3.78	3.95	1.67	1.32
Trend-based precipitation change (%) ^b	+2.2	+0.8	−8.5	−9.1	−13	−10	−8.0
	Above LYX	LYX to LZ	LZ to TDG	TDG to LM	LM to SMX	SMX to HYK	Below HYK
Length of stream segment (km)	1684	412	1376	723	275	208	786
Catchment area (10 ³ km ²)	131	92	134	130	201	31.8	21.9
Water consumption per unit area (10 ³ m ³ /km ²) ^c	1.5	28	93	10	39	86	537

^a Period average (1957–2016). ^b $(P_{W2016} - P_{W1957})/P_{W1957} \times 100$, where P_{W2016} and P_{W1957} are trend-based precipitation water in 2016 and 1957. ^c Period average (1998–2016). TNH: Tangnaihahai; LZ: Lanzhou; TDG: Toudaoguai; LM: Longmen; TG: Tongguan; HYK: Huayuankou; LJ: Lijin; LYX: Longyangxia; SMX: Sanmenxia.

Table A6. Downstream and temporal increases in population, grain yield and GDP per unit area in the Yellow River Basin.

		Headwater Areas	Upper Reaches	Middle Reaches	Lower Reaches
Population density (p/km ²)	1957–1966	2.5	19	94	339
	2007–2016	4.5	46	183	602
	Growth	2.0	27	89	269
Grain yield per unit area (t/km ²)	1957–1966	0.7	5.2	22	71
	2007–2016	1.3	24.4	73	308
	Growth	0.6	19	52	237
GDP per unit area (10 ³ USD/km ²)	1957–1966	0.06	0.58	3.62	6.09
	2007–2016	21.7	203	1267	3623
	Growth	21.7	202	1263	3617

Headwater: Above Tangnaihahai. Upper reaches: Between Tangnaihahai and Toudaoguai. Middle reaches: Between Toudaoguai and Huayuankou. Lower reaches: Between Huayuankou and Lijin).

References

1. Creed, I.F.; Lane, C.R.; Serran, J.N.; Alexander, L.C.; Basu, N.B.; Calhoun, A.J.K.; Christensen, J.E.; Cohen, M.J.; Craft, C.; D'Amico, E.; et al. Enhancing protection for vulnerable waters. *Nat. Geosci.* **2017**, *10*, 809–815. [[CrossRef](#)] [[PubMed](#)]
2. Hering, J.G.; Ingold, K.M. Water resources management: What should be integrated? *Science* **2012**, *336*, 1234–1235. [[CrossRef](#)] [[PubMed](#)]
3. Larsen, T.A.; Hoffmann, S.; Lüthi, C.; Truffer, B.; Maurer, M. Emerging solutions to the water challenges of an urbanizing world. *Science* **2016**, *352*, 928–933. [[CrossRef](#)] [[PubMed](#)]
4. Vörösmarty, C.J.; McIntyre, P.B.; Gessner, M.O.; Dudgeon, D.; Prusevich, A.; Green, P.; Glidden, S.; Bunn, S.E.; Sullivan, C.A.; Reidy Liermann, C. Global threats to human water security and river biodiversity. *Nature* **2010**, *467*, 555–561. [[CrossRef](#)]

5. Wiegel, R.L. Nile delta erosion. *Science* **1996**, *272*, 338–340. [[CrossRef](#)]
6. Milliman, J.D.; Farnsworth, K.L. *River Discharge to the Coastal Ocean*; Cambridge University Press: Cambridge, UK, 2011.
7. Milly, P.C.D.; Dunne, K.A.; Vecchia, A.V. Global pattern of trends in streamflow and water availability in a changing climate. *Nature* **2005**, *438*, 347–350. [[CrossRef](#)]
8. Arnell, N.W. Climate change and global water resources: SRES emissions and socio-economic scenarios. *Glob. Environ. Chang.* **2004**, *14*, 31–52. [[CrossRef](#)]
9. Piao, S.; Ciais, P.; Huang, Y.; Shen, Z.; Peng, S.; Li, J.; Zhou, L.P.; Liu, H.Y.; Ma, Y.C.; Ding, Y.H.; et al. The impacts of climate change on water resources and agriculture in China. *Nature* **2010**, *467*, 43–51. [[CrossRef](#)]
10. Schewe, J.; Heinke, J.; Gerten, D.; Haddeland, I.; Arnell, N.W.; Clark, D.B.; Dankers, R.; Eisner, S.; Fekete, B.M.; Colón-González, F.J.; et al. Multimodel assessment of water scarcity under climate change. *Proc. Natl. Acad. Sci. USA* **2014**, *111*, 3245–3250. [[CrossRef](#)]
11. Sun, Q.; Miao, C.; Duan, Q.; Ashouri, H.; Sorooshian, S.; Hsu, K. A Review of Global Precipitation Data Sets: Data Sources, Estimation, and Intercomparisons. *Rev. Geophys.* **2018**, *56*, 79–107. [[CrossRef](#)]
12. Vörösmarty, C.J.; Green, P. Global Water Resources: Vulnerability from Climate Change and Population Growth. *Science* **2000**, *289*, 284–289. [[CrossRef](#)] [[PubMed](#)]
13. Oki, T.; Kanae, S. Global hydrological cycles and world water resources. *Science* **2006**, *313*, 1068–1072. [[CrossRef](#)] [[PubMed](#)]
14. Liu, C.; Zhang, X. Causal Analysis on Actual Water Flow Reduction in the Mainstream of the Yellow River. *Acta Geogr. Sin.* **2004**, *59*, 323–330.
15. Jiang, C.; Xiong, L.; Wang, D.; Liu, P.; Guo, S.; Xu, C.Y. Separating the impacts of climate change and human activities on runoff using the Budyko-type equations with time-varying parameters. *J. Hydrol.* **2015**, *522*, 326–338. [[CrossRef](#)]
16. Gao, Z.; Zhang, L.; Zhang, X.; Cheng, L.; Potter, N.; Cowan, T.; Cai, W. Long-term streamflow trends in the middle reaches of the Yellow River Basin: Detecting drivers of change. *Hydrol. Process.* **2016**, *30*, 1315–1329. [[CrossRef](#)]
17. Wang, Y.; Zhao, W.; Wang, S.; Feng, X.; Liu, Y. Yellow River water rebalanced by human regulation. *Sci. Rep.* **2019**, *9*, 9707. [[CrossRef](#)]
18. Wang, H.; Yang, Z.; Saito, Y.; Liu, J.P.; Sun, X.X. Interannual and seasonal variation of the Huanghe (Yellow River) water discharge over the past 50 years: Connections to impacts from ENSO events and dams. *Glob. Planet. Chang.* **2006**, *50*, 212–225. [[CrossRef](#)]
19. Li, B.; Li, C.; Liu, J.; Zhang, Q.; Duan, L. Decreased Streamflow in the Yellow River Basin, China: Climate Change or Human-Induced? *Water* **2017**, *9*, 116. [[CrossRef](#)]
20. Gao, P.; Mu, X.-M.; Wang, F.; Li, R. Changes in streamflow and sediment discharge and the response to human activities in the middle reaches of the Yellow River. *Hydrol. Earth Syst. Sci.* **2011**, *15*, 1–10. [[CrossRef](#)]
21. Miao, C.Y.; Ni, J.R.; Borthwick, A.G.L. Recent changes of water discharge and sediment load in the Yellow River basin, China. *Prog. Phys. Geogr.* **2010**, *34*, 541–561. [[CrossRef](#)]
22. Zhao, G.; Li, e.; Mu, X.; Wen, Z.; Rayburg, S.; Tian, P. Changing trends and regime shift of streamflow in the Yellow River basin. *Stoch. Environ. Res. Risk Assess.* **2015**, *29*, 1331–1343. [[CrossRef](#)]
23. Chen, J.W. Tendency, causes and control measures on Yellow River dry-up. *J. Nat. Resour.* **2000**, *15*, 31–35.
24. Yao, W.; Zhao, Y.; Tang, L.; Li, S. Preliminary study on no flow disaster in the lower reaches of Yellow River. *Adv. Water Sci.* **1999**, *10*, 160–164.
25. Peng, K. China water resource crisis in the 21th century. *Adv. Sci. Technol. Water Resour.* **2000**, *20*, 13–16.
26. He, C. Route and Model Towards a Great Modernized Country. *Bull. Chin. Acad. Sci.* **2018**, *33*, 274–283.
27. Li, Q.J.; Liu, Z.S.; Xiao, S.J.; Meng, J. Water demand prediction of national economy in the Yellow River Basin. *Yellow River* **2011**, *33*, 61–63.
28. Dey, P.; Mishra, A. Separating the impacts of climate change and human activities on streamflow: A review of methodologies and critical assumptions. *J. Hydrol.* **2017**, *548*, 278–290. [[CrossRef](#)]
29. Yang, S.L.; Xu, K.H.; Milliman, J.D.; Yang, H.F.; Wu, C.S. Decline of Yangtze River water and sediment discharge: Impact from natural and anthropogenic changes. *Sci. Rep.* **2015**, *5*, 12581. [[CrossRef](#)]
30. Yang, H.F.; Yang, S.L.; Xu, K.H.; Milliman, J.D.; Wang, H.; Yang, Z.; Chen, Z.; Zhang, C.Y. Human impacts on sediment in the Yangtze River: A review and new perspectives. *Glob. Planet. Chang.* **2018**, *162*, 8–17. [[CrossRef](#)]

31. Mann, H.B. Nonparametric Tests Against Trend. *Econometrica* **1945**, *13*, 245–259. [CrossRef]
32. Kendall, M.G. *Rank Correlation Methods*; Charles Griffin: London, UK, 1975.
33. Meade, R.H.; Moody, J.A. Causes for the decline of suspended-sediment discharge in the Mississippi River system, 1940–2007. *Hydrol. Process.* **2010**, *24*, 35–49. [CrossRef]
34. Yang, S.L.; Liu, Z.; Dai, S.B.; Gao, Z.X.; Zhang, J.; Wang, H.J.; Luo, X.X.; Wu, C.S.; Zhang, Z. Temporal variations in water resources in the Yangtze River (Changjiang) over the Industrial Period based on reconstruction of missing monthly discharges. *Water Resour. Res.* **2010**, *46*, W10516. [CrossRef]
35. Dai, S.B.; Yang, S.L.; Cai, A.M. Catena Impacts of dams on the sediment flux of the Pearl River, southern China. *Catena* **2008**, *76*, 36–43. [CrossRef]
36. Liu, C.; Wang, S.; Liang, Y.; Leung, R.L. Analysis of Pan Evaporation Change and the Influence Factors in the Yellow River Basin in 1961–2010. *Progress. Inquisitiones Mutat. Clim.* **2013**, *9*, 327–334.
37. Roderick, M.L.; Farquhar, G.D. The cause of decreased pan evaporation over the past 50 years. *Science* **2002**, *298*, 1410–1411. [PubMed]
38. Lu, D. History of irrigation in Ningxia Plain. *Yellow River* **1990**, *12*, 69–72.
39. Ministry of Water Resources of China (MWRRC). China Water Resources Bulletin in 1997–2016. Available online: <http://www.mwr.gov.cn/sj/tjgb/szygb/> (accessed on 1 July 2019). (In Chinese)
40. Dai, S.B.; Yang, S.L.; Li, M. Sharp decrease in suspended sediment supply from China's rivers to the sea: Anthropogenic and natural causes. *Hydrolog. Sci. J.* **2009**, *54*, 135–146. [CrossRef]
41. Yellow River Conservancy Commission (YRCC). Yellow River Water Resource Bulletin in 2016. Available online: <http://www.yrcc.gov.cn/other/hhgb/2016szygb/index.html#p=1> (accessed on 1 July 2019). (In Chinese)
42. Wang, H.; Wu, X.; Bi, N.; Li, S.; Yuan, P.; Wang, A.; Syvitski, J.P.M.; Saito, Y.; Yang, Z.; Liu, S. Impacts of the dam-orientated water-sediment regulation scheme on the lower reaches and delta of the Yellow River (Huanghe): A review. *Glob. Planet. Chang.* **2017**, *157*, 93–113. [CrossRef]
43. Feng, X.; Fu, B.; Piao, S.; Wang, S.; Zeng, Z.; Lü, Y.; Zeng, Y.; Li, Y. Revegetation in China's loess plateau is approaching sustainable water resource limits. *Nat. Clim. Chang.* **2016**, *6*, 1019. [CrossRef]
44. Lv, M.; Ma, Z.; Li, M.; Zheng, Z. Quantitative analysis of terrestrial water storage changes under the grain for green program in the Yellow River Basin. *J. Geophys. Res. Atmos.* **2019**, *124*, 1336–1351. [CrossRef]
45. Xu, J. Effect of human activities on overall trend of sedimentation in the lower Yellow River, China. *Environ. Manag.* **2004**, *33*, 637–653.
46. Chen, L.Q.; Liu, C.M. Influence of climate and land-cover change on runoff of the source regions of Yellow River. *China Environ. Sci.* **2007**, *27*, 559–565.
47. Qiu, G.Y.; Yin, J.; Xiong, Y.J.; Zhao, S.H.; Wang, P.; Wu, X.Q.; Zeng, S. Studies on the Effects of Climatic warming-drying trend and land use change on the runoff in the Jinghe River Basin. *J. Nat. Resour.* **2008**, *23*, 211–218.
48. Zheng, H.; Zhang, L.; Zhu, R.; Liu, C.; Sato, Y.; Fukushima, Y. Responses of streamflow to climate and land surface change in the headwaters of the Yellow River Basin. *Water Resour. Res.* **2009**, *45*, W00A19. [CrossRef]
49. Shi, P.; Wang, J.; Feng, W.; Ye, T.; Ge, Y.; Chen, J.; Liu, J. Response of eco-environmental security to land use/cover changes and adjustment of land use policy and pattern in China. *Adv. Earth Sci.* **2006**, *21*, 111–119.
50. Ministry of Land and Resources of China (MLRC). China Land and Resources Bulletin in 2016. Available online: <https://wenku.baidu.com/view/cd4d0610657d27284b73f242336c1eb91b373351.html> (accessed on 1 July 2019). (In Chinese).
51. Liu, C.; Zheng, H. Trend analysis of hydrological components in the Yellow River basin. *J. Nat. Resour.* **2003**, *18*, 130–135.
52. Zhang, Q.; Xu, C.Y.; Yang, T. Variability of water resource in the Yellow River Basin of past 50 years, China. *Water Resour. Manag.* **2009**, *23*, 1157–1170. [CrossRef]
53. Stocker, T.F.; Qin, D.; Plattner, G.K.; Tignor, M.M.B.; Allen, S.K.; Boschung, J.; Nauels, A.; Xia, Y.; Bex, V.; Midgley, P.M. *Climate Change 2013: The Physical Science Basis*; Cambridge University Press: Cambridge, UK, 2013.
54. Tian, Q.; Yang, S. Regional climatic response to global warming: Trends in temperature and precipitation in the Yellow, Yangtze and Pearl River basins since the 1950s. *Quat. Int.* **2017**, *440*, 1–11. [CrossRef]
55. Xue, S. Summary of Yellow River Basin Integrated Water Resources Plan. *China Water Resour.* **2011**, *23*, 108–111.

56. Wang, B.C.; Liu, H.M.; Xu, L.J. Demonstration and Determination of the Main Technical Indicators of Soil and Water Conservation Planning of Yellow River Basin. *Yellow River* **2013**, *35*, 127–130.
57. Carriquiry, J.D.; Sánchez, A. Sedimentation in the Colorado River delta and Upper Gulf of California after nearly a century of discharge loss. *Mar. Geol.* **1999**, *158*, 125–145. [[CrossRef](#)]
58. Patil, R.; Wei, Y.; Pullar, D.; Shulmeister, J. Understanding hydro-ecological surprises for riverine ecosystem management. *Curr. Opin. Environ. Sustain.* **2018**, *33*, 142–150. [[CrossRef](#)]
59. Stanley, D.J.; Warne, A.G. Nile Delta: Recent Geological Evolution and Human Impact. *Science* **1993**, *260*, 628–634. [[CrossRef](#)] [[PubMed](#)]
60. Zhang, Q.; Yang, Z.; Hao, X.; Ping, Y. Conversion features of evapotranspiration responding to climate warming in transitional climate regions in northern China. *Clim. Dyn.* **2019**, *52*, 3891–3903. [[CrossRef](#)]
61. Li, H. Feasibility analysis of “Sky River Project” based on manual intervention of transport track. *Jiangsu Sci. Technol. Inf.* **2019**, *36*, 73–76.
62. Giosan, L.; Syvitski, J.; Constantinescu, S.; Day, J. Climate change: Protect the world’s deltas. *Nature* **2014**, *516*, 31. [[CrossRef](#)]
63. Humborg, C.; Ittekkot, V.; Cociasu, A.; Bodungen, B.V. Effect of Danube River dam on Black Sea biogeochemistry and ecosystem structure. *Nature* **1997**, *386*, 385–388. [[CrossRef](#)]
64. Syvitski, J.P.M.; Vörösmarty, C.J.; Kettner, A.J.; Pamela, G. Impact of humans on the flux of terrestrial sediment to the global coastal ocean. *Science* **2005**, *308*, 376–380. [[CrossRef](#)]
65. Pereira, E.; Quintella, B.R.; Mateus, C.S.; Alexandre, C.M.; Belo, A.F.; Telhado, A.; Quadrado, M.F.; Almeida, P.R. Performance of a Vertical-Slot Fish Pass for the Sea Lamprey *Petromyzon marinus* L. and Habitat Recolonization: Performance of a Fish Pass for Sea Lamprey. *River Res. Appl.* **2016**, *33*, 16–26. [[CrossRef](#)]
66. Wang, S.; Fu, B.; Piao, S.; Lü, Y.; Ciais, P.; Feng, X.; Wang, Y. Reduced sediment transport in the Yellow River due to anthropogenic changes. *Nat. Geosci.* **2016**, *9*, 38–42. [[CrossRef](#)]
67. Chu, Z.X.; Sun, X.G.; Zhai, S.K.; Xu, K.H. Changing pattern of accretion/erosion of the modern Yellow River (Huanghe) subaerial delta, China: Based on remote sensing images. *Mar. Geol.* **2006**, *227*, 13–30. [[CrossRef](#)]
68. Cui, B.; Yang, Q.; Yang, Z.; Zhang, K. Evaluating the ecological performance of wetland restoration in the Yellow River Delta, China. *Ecol. Eng.* **2009**, *35*, 1090–1103. [[CrossRef](#)]
69. Wang, M.; Qi, S.; Zhang, X. Wetland loss and degradation in the Yellow River Delta, Shandong Province of China. *Environ. Earth Sci.* **2012**, *67*, 185–188. [[CrossRef](#)]
70. Fan, H.; Huang, H. Response of coastal marine eco-environment to river fluxes into the sea: A case study of the Huanghe (Yellow) River mouth and adjacent waters. *Mar. Environ. Res.* **2008**, *65*, 378–387. [[CrossRef](#)]
71. Li, F.; Zhang, X. Impact of human activity on “Marine Big Environment” and protective tactics. *Mar. Sci.* **2000**, *24*, 6–8.
72. Wang, B.; Ding, Q. Changes in global monsoon precipitation over the past 56 years. *Geophys. Res. Lett.* **2006**, *33*, 272–288. [[CrossRef](#)]
73. Choudhury, B.J. Global pattern of potential evaporation calculated from the Penman-Monteith equation using satellite and assimilated data. *Remote Sens. Environ.* **1997**, *61*, 64–81. [[CrossRef](#)]
74. Foley, J.A.; DeFries, R.; Asner, G.P.; Barford, C.; Bonan, G.; Carpenter, S.R.; Chapin, F.S.; Coe, M.T.; Daily, G.C.; Gibbs, H.K.; et al. Global consequences of land use. *Science* **2005**, *309*, 570–574. [[CrossRef](#)]
75. Gocic, M.; Trajkovic, S. Analysis of changes in meteorological variables using Mann-Kendall and Sen’s slope estimator statistical tests in Serbia. *Glob. Planet. Chang.* **2013**, *100*, 172–182. [[CrossRef](#)]
76. Wu, C.S.; Yang, S.L.; Lei, Y.P. Quantifying the anthropogenic and climatic impacts on water discharge and sediment load of the Pearl River (Zhujiang), China (1954–2009). *J. Hydrol.* **2012**, *452*, 190–204. [[CrossRef](#)]
77. Jia, J. *Dam Construction in China*; China Water and Power Press: Beijing, China, 2013.

